

# We are IntechOpen, the world's leading publisher of Open Access books Built by scientists, for scientists

4,800

Open access books available

122,000

International authors and editors

135M

Downloads

Our authors are among the

154

Countries delivered to

TOP 1%

most cited scientists

12.2%

Contributors from top 500 universities



WEB OF SCIENCE™

Selection of our books indexed in the Book Citation Index  
in Web of Science™ Core Collection (BKCI)

Interested in publishing with us?  
Contact [book.department@intechopen.com](mailto:book.department@intechopen.com)

Numbers displayed above are based on latest data collected.  
For more information visit [www.intechopen.com](http://www.intechopen.com)



# Frequency-Power Control of VSWG for Improved Frequency Regulation

*Asma Aziz and Aman Than Oo*

## Abstract

With increasing wind energy penetration and impending grid codes, it is important to enable wind-based power plants to provide sensitive frequency response in grids that may experience irregular frequency fluctuations with noise induced. Transient low-frequency deviations are handled by inertial control, while active power frequency response controller is needed for high-frequency control. A frequency processor-based frequency-active power set point controller architecture for variable speed wind turbine generator (VSWG) is presented in this paper. Grid frequency processor based on moving averaged frequency and dynamic dead-band is tested for two different grid codes. Generated active power set point is provided to a modified torque-pitch control loop in type 3 and type 4 variable speed wind turbine generator generic models. Delay model of hydro system in a single area load frequency control is applied to investigate frequency support from proposed frequency response controller-based VSWG. Area frequency response along with VSWG electrical power support is compared with other droop-based VSWG model to establish the superiority of proposed frequency-active power controller-based VSWG over other droop-based VSWG models.

**Keywords:** frequency response, VSWG, active power control, frequency grid code, load frequency control

## 1. Introduction

Deteriorating power quality due to frequency variations can pose risk of severe economic impacts on a big interconnected electrical network like Australian national electricity market (NEM). In case of rare contingency event like that of 2009 blackout in Victoria [1], load shedding at high level is permissible for frequency regulation and electrical system stability, but for control area like South Australia having wind penetration as high as 70% in some of the days or islanding-prone area like Tasmania, regular load shedding is not acceptable due to high-frequency excursions. Frequency regulation is imperative when ratio of highest contingency loss to system size is relatively high. For large interconnected network like NEM, this ratio is low, but for state network like Tasmania or South Australia where islanding probability is more and there has high wind penetration, frequency regulation from participating frequency-responsive generating plants is highly important on a daily basis.

System frequency is regulated by injecting active power into electric grid through power plants. This control is indispensable for stable operation of grid ensuring continuous adaptation of generation to demand. Under a wide range of ambient conditions, frequency-responsive power plants are expected to provide automatic power variation with frequency deviation within a given time frame and ramp limit. The conventional power plants which remain connected to grid even in case of frequency deviations accomplish active power-frequency control through turbine governors' reaction to nominal synchronous speed deviations and the respective boiler-turbine frequency-responsive controls. Dead-band and speed droop are two significant parameters in conventional turbine governor action during system event [2]. Long-term system frequency regulation fidelity is highly dependent upon implemented dead-band. Governor dead-band is detrimental to minimum frequency variation needed before the governor action is activated. The relative frequency deviation with respect to the relative change in power output defined as speed droop is always positive for stable regulation. Factors like available headroom, maximum-minimum power capacity of generating units, and power set point enabling frequency operating modes directly affect the total frequency-responsive reserve amount. A generator operating at its maximum generating capacity has almost negligible headroom and is therefore unable to provide any frequency-responsive operation irrespective of governor droop being enabled.

In order to get an emulated synchronous generator-like response, abovementioned parameters like droop, dead-band, and headroom are needed to be considered in variable speed wind turbine generator (VSWTG) generic modeling for frequency-active power control. The generic models are functional models appropriate for the investigation with lower simulation period for large-scale power systems. These generic models can sufficiently represent all dynamics associated with the impact of active power variations in the time range of 50 ms to 100 min. Based on trends in the connection process globally, doubly fed induction generator-based type 3 and full converter-based type 4 VSWTG are dominating renewable energy market. Different type 3 VSWTG models [3–5] exist in literature studies, but wind turbine and wind power plant (WPP) model still lack standardization, and works are in progress. Various software like PSLF, PSS-E, DlgSILENT, etc., have been used for implementing these models. An official version of second generation WECC models was released in 2014, but their adoption has not been up to the desired level as not every type of VSWTG model can be applied in every study [6]. Even though VSWTG model characterization development has been fundamentally accomplished, development of plant controllers especially regarding frequency response control is still under developing stage.

The impending system inertia reduction with increased integration of power electronics-based wind power plants has led transmission system operators (TSO) to establish new grid codes for frequency-based ancillary services from wind farms in big interconnected electrical grid. Grid codes like that of the UK [7] require a response from wind farms under normal conditions and limited up/down response under high-frequency conditions. In case of TSO commanded restriction on active power output, Irish grid code implies all grid-integrated generating units to be capable of operating at a reduced output level. According to Australia's national electricity market (NEM), it is compulsory for generators  $\geq 30$  MW to participate in frequency control ancillary services [8]. Operation of the VSWTGs in maximum power tracking mode results in zero spinning reserve for utilization in frequency regulation. In view of compulsory grid code frequency support, this power electronics-based VSWTG requires modified active power control algorithm to support regulation services. Frequency-active power control model is an auxiliary control algorithm implemented in individual wind turbine generator control loop for providing controllable power reserve on

demand in the form of spinning reserve or power ramp rate limit to respond to system frequency deviations. Wind turbine active power frequency regulation analysis has received considerable research focus in the form of inertial control and primary frequency control analysis either at individual wind turbine level or at wind farm level [9–14]. Most of the past researches focus on modifying individual turbine control algorithm for analyzing primary frequency control capabilities from wind turbines. These algorithms focus on either achieving de-loaded performance [15–18] to enhance VSWTG’s frequency regulation capability or investigated feasibility of droop control on frequency stability [19–24]. The basic idea behind most of the droop-based studies for emulating primary frequency response and inertial response studies is to add an additional signal, sensitive to frequency to the speed or torque controller which appears as reference power set point in VSWTG model, thereby momentarily increasing the wind turbine output power. However, the output reference power set points from these controls are not grid code compatible.

Power set points are the target for required electrical energy generation from wind plants. These targets can be based on available wind, operational mode, or required frequency response. Active power set point characteristics and the expected behavior of the different generating units under different set points are defined in country-specific grid codes. Centralized wind farm control for active power set point distribution to individual turbines from wind farm controller was presented in [25]. In this model, wind turbines receive power set point distributed through a centralized wind farm controller which is provided by transmission system operator, and wind turbines did not individually respond to frequency excursions at their terminals. Another research study for active power control of wind turbine presented a control system for tracking a power reference and provides a primary frequency response with constant droop in the absence of any dead-band with diminishing turbine structure loading [26]. [27] describes three de-rating command mode for wind turbine operation as  $DR_{cmd}P_{rated}$ ,  $P_{avail} - (1 - DR_{cmd})P_{rated}$ , and  $DR_{cmd}P_{avail}$ , where  $DR_{cmd}$  is the de-rating command set point,  $P_{rated}$  is rated output of wind plant, and  $P_{avail}$  is the available wind power. In another study, three different operating modes (de-rated, absolute spinning reserve, and relative spinning reserve) [28] are defined. As an example, operating mode 1 is defined as de-rated or normal such that:

$$P_{ref} = \left\{ \begin{array}{l} P_{operator} \quad \forall P_{operator} \leq P_{avail} \\ P_{avail} \quad \forall P_{avail} \leq P_{operator} \end{array} \right\}$$

In the view of above discussions, the objectives of the current paper are as follows:

1. To present a grid frequency processor scheme based on dynamic dead-band around moving averaged frequency instead of conventional static dead-band for generation of continuously varying, frequency-sensitive active power reference set point for VSWTG and its corresponding effect on system primary frequency control.
2. Frequency-sensitive response and frequency limited sensitive response are explored through dynamic dead-band concept and nonsymmetrical droop for power variation at wind turbine level.
3. Grid code-sensitive frequency active power controller-based type 3 and type 4 wind turbine response is analyzed with response of frequency-dependent linear droop controller-based wind turbine generator model.

4. Frequency controllers' performance is compared with and without wind power in algorithm.

This paper is structured in the following sections. Section 2 explains the modeling of grid code-sensitive frequency controller for active power response in VSWTG. Individual blocks including grid frequency processor highlighting effect of variation of dead-band and wind turbine control loop are explained. Section 3 discusses test system load frequency control model incorporating hydro power plant and frequency-responsive power wind power plant. MATLAB-based simulation results are used to compare frequency response controller I- and frequency response controller II-based VSWTG response.

## 2. Grid code-sensitive frequency controller for active power response in VSWTG

### 2.1 Dead-band: static vs. dynamic

Generator droop characteristic means that generating unit will inversely change power output level in proportion to system frequency. Responding to frequency deviations, generating units depart from their dispatch targets according to the set droop characteristics. This droop behavior can be avoided by implementing a dead-band on each unit. Static dead-band is thus a symmetrical buffer zone on either side of 50/60 Hz frequency that compensates for frequency noise. Droop response of generating machine from controlling power output of machine is avoided when frequency lies within the upper and lower dead-band range. Dynamic dead-band incorporates a buffer zone on either side of moving averaged frequency signal instead of nominal frequency signal. Both these dead-bands are represented in **Figure 1**.

### 2.2 Grid frequency processor background

Providing grid frequency directly to wind turbine controller will generate noise-induced frequency-sensitive active power set point. This will result in noisy output power, thus providing frequency response for any frequency error even due to grid noise. Noisy power output will have an adverse effect on supplied power quality

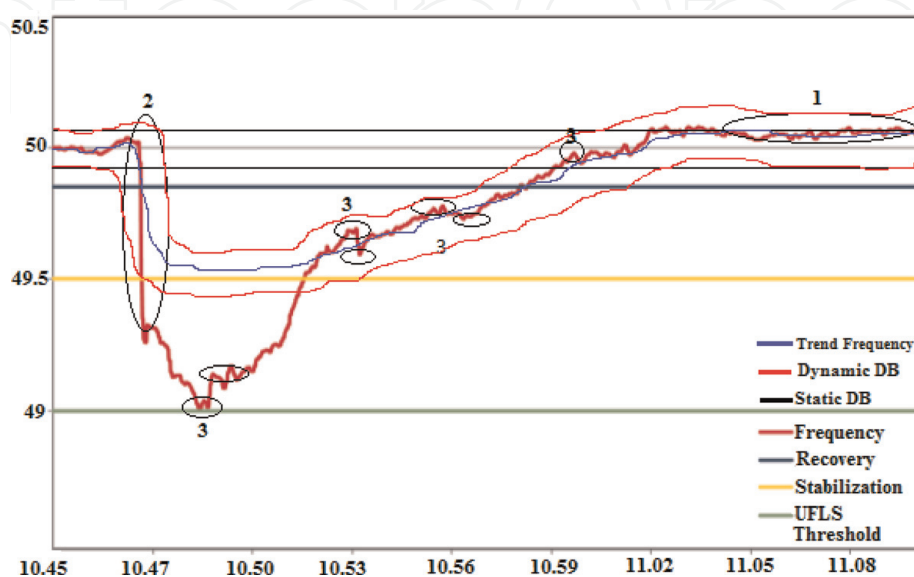


**Figure 1.**  
NEM mainland frequency 1045–1109 h during a contingency event [1].

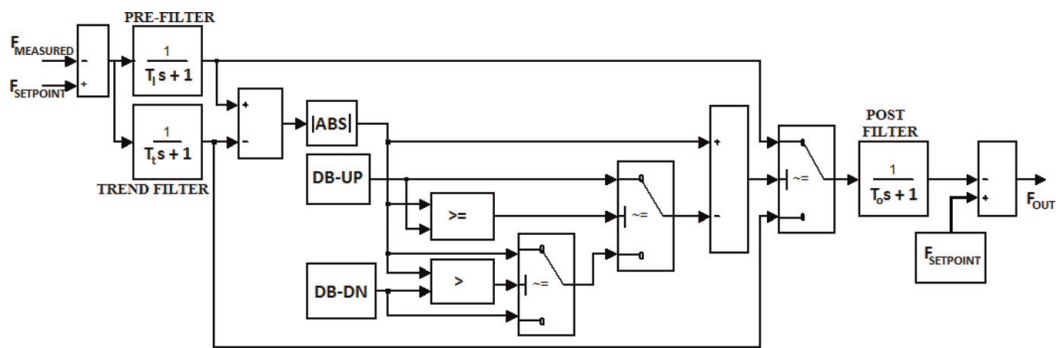


**Figure 2.**  
 Basic structure of grid frequency processor.

and turbine life. An analysis of electrical grid dynamics can serve as the base of grid processing system for distinguishing different types of frequency signals. **Figure 2** shows NEM mainland real frequency trace during 2009 contingency event when 3205 MW of total generation disconnected automatically, resulting in under frequency load shedding across the Australian NEM interconnected system [1].

Though we could not get enough data points to represent a very clear picture here, but still three different frequency signals 1, 2, and 3 as defined below can be distinguished in **Figure 1**. Electrical grid frequency signal can be considered as composition of three types of signals [29]:

1. Low ramping signals arising due to normal trend of generation-demand and grid dynamics over long term of several minutes
2. High-amplitude, high-frequency range during contingency which is normally low in occurrence
3. Low-amplitude signals in high-frequency range due to stochastic grid noise with high occurrence rate

First two signals have very low effect on turbine life, while highly occurring type 3 noise signals have ample effect on turbine life time and should be suppressed. A closer look at **Figure 1** shows that trend frequency signals 1 are usually around the static dead-band, while high-amplitude signal 2 is always outside the static dead-band. Discerning these signals just on the basis of frequency through filters is not a viable option as they are present in whole frequency signal over a time period. Implementing a dynamic dead-band centered around the trend frequency signal in a grid processing system would distinguish these types of signals.

### 2.3 Frequency processor model

A grid frequency processing system centered around moving averaged frequency signal was proposed in [29]. A modified version of the frequency processor is implemented in current study for utilization in active power set point controller for variable speed wind turbine generator system operating under frequency-responsive mode. Basic structure of grid frequency processor block which provides dynamic dead-band-based processed frequency output is shown in **Figure 2**. Frequency processor takes grid frequency at PCC and nominal frequency (50 or 60 Hz) as input signal. Three low-pass filters and dead-band constitute the processor model. Moving average of the measured grid frequency is termed as a trend frequency which characterizes long-term behavior of grid frequency. The theoretical moving average filter (MAF) is mathematically expressed as

$$y[i] = \frac{1}{M} \sum_{j=0}^{M-1} x[i+j] \quad (1)$$

where  $x$  is the input frequency signal,  $y$  is the output frequency signal, and  $M$  is the number of points in average [30]. A moving average filter will cause minimal change to a signal whose period is long compared to the filter window length, because the filter's window only "sees" a small and relatively constant part of the oscillating signal at each moment. MAF, which can be practically implemented as the finite impulse response filter (FIR), produces lowest noise component in output signal by equally treating all incoming signal.

A simple moving average filter acts as a low-pass filter. A low-pass filter passes very low frequencies with minimal change, but it reduces the amplitude of high-frequency signals or of high-frequency components in a complex signal. A low-pass filter with a cutoff of  $f_{CO} = 0.443/T_t$  has been used to act as MAF to construct trend frequency in this study. Trend frequency is assumed to lie within the dead-band, so selecting the trend filter time constant between 8 and 30 s will provide a cutoff frequency  $50 \pm 0.015$  to  $50 \pm 0.05$  Hz. The time constant for prefilter is taken as 0.5 s which gives a cutoff frequency of  $50 \pm 0.89$  Hz. This time constant will ensure filtering under normal frequency variation just before the under-frequency load shedding (UFLS) as shown in **Figure 1**. Trend frequency signal is subtracted from prefiltered measured frequency, and resulting absolute frequency difference is then passed through dead-band algorithm. The dead-band algorithm dynamically limits the range of the input signal according to the upper and lower dead-band limits. If  $DB-UP \leq |F_{Filter} - F_{trend}| > DB-DN$ , output is set to zero. If  $|F_{Filter} - F_{trend}| > DB-UP$ , the output appears as the input shifted down by the DB-UP. If  $|F_{Filter} - F_{trend}| < DB-DN$ , output appears as input signal shifted down by the DB-DN, as indicated in **Figure 3**.

Flowchart for basic frequency processor algorithm is shown in **Figure 3**. **Figure 4** shows the measured grid frequency and processed out frequency for different threshold values for selector switch. These threshold values are selected based on different upper and lower dead-band limits. For example, for a system with dead-band limit of  $\pm 0.03$  Hz, threshold is selected as 0.03. In this study, an upper dead-band of 0.015 Hz which is the standard value for most of the TSO [31, 32] and lower dead-band of 0.001 Hz are selected, so 0 is selected as the threshold value. As per NERC policy, total dead-band applied should be limited to 0.035 [33].

Output processed frequency is basically composition of trend frequency and measured filtered frequency as seen in **Figure 5**. We can notice output processed frequency in black color following trend frequency in green color most of the time when dead-band output is zero, while processed frequency follows measured frequency in red color whenever threshold increases above zero. As stated previously, frequency processor is dependent upon implemented threshold value and dead-band limits which can be set as per TSO requirements.

A 14-generator NEM model is a simplified model of the eastern and southern 50 Hz Australian electrical networks, which was originally proposed for small-signal stability studies [34]. In the original model, there are 14 generators, 5 static VAR compensators (SVCs), 59 busses, and 104 lines with voltage levels ranging from 15 to 500 kV. It is assumed that all thermal and hydro power plants have a standard steam turbine governor (i.e., IEEEG1) and hydro turbine governor (i.e., HYGOV), respectively. **Figure 6** presents the grid frequency from one of the busses from NEM model which is provided to grid frequency processor. The resulting processed and filtered frequency is shown in **Figure 7**. The next section discusses the application of grid frequency processor in different types of frequency controllers for generating frequency-sensitive power set points.

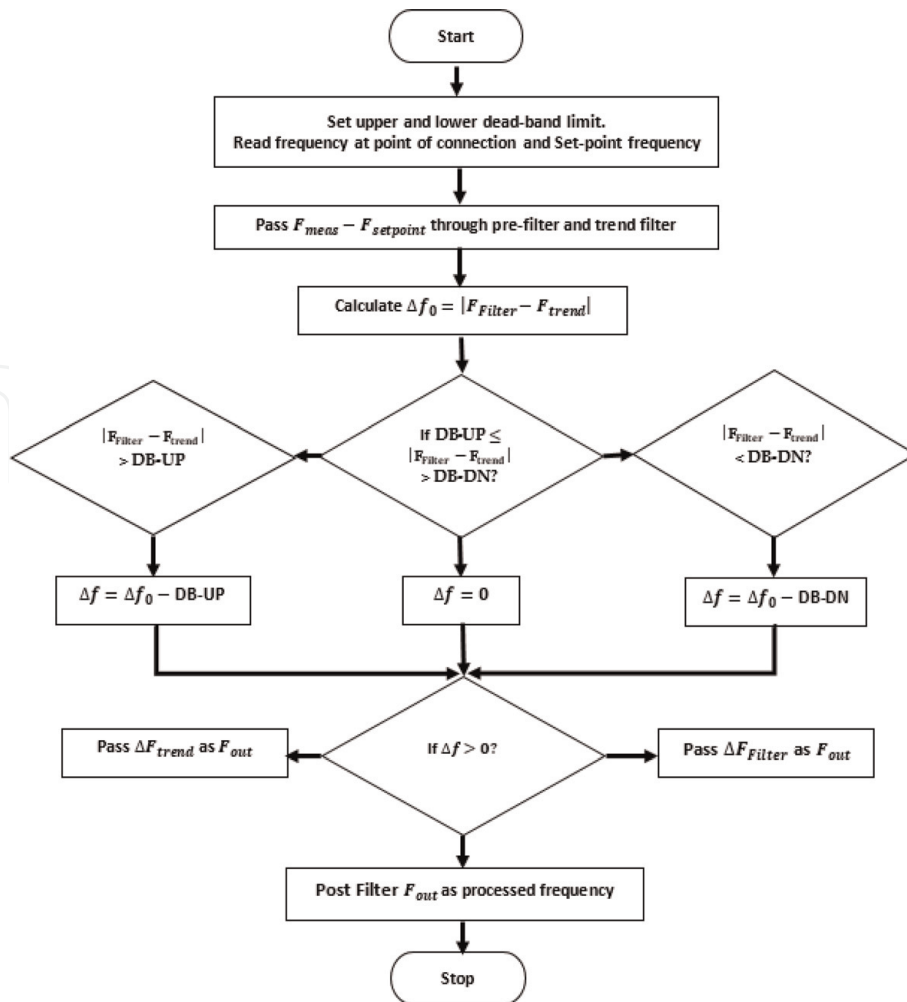


Figure 3.  
 Algorithm for grid frequency processor.

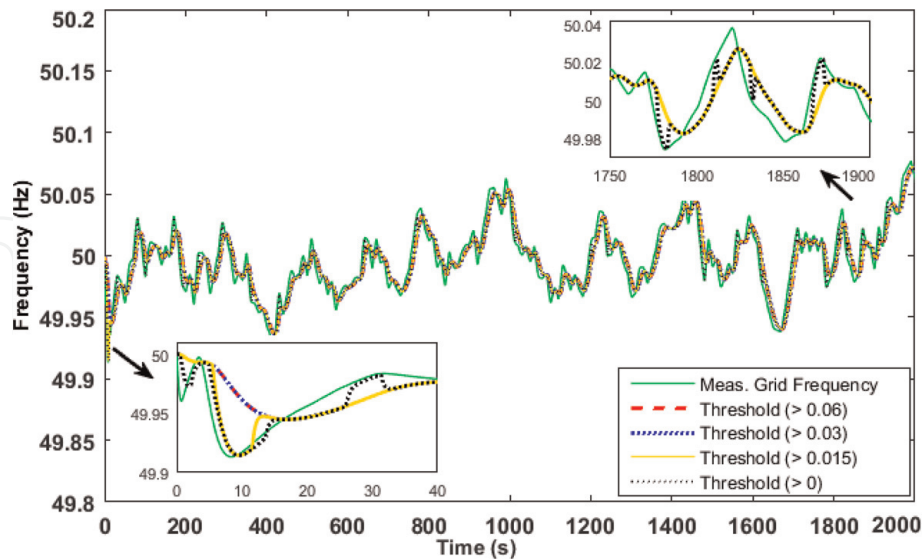
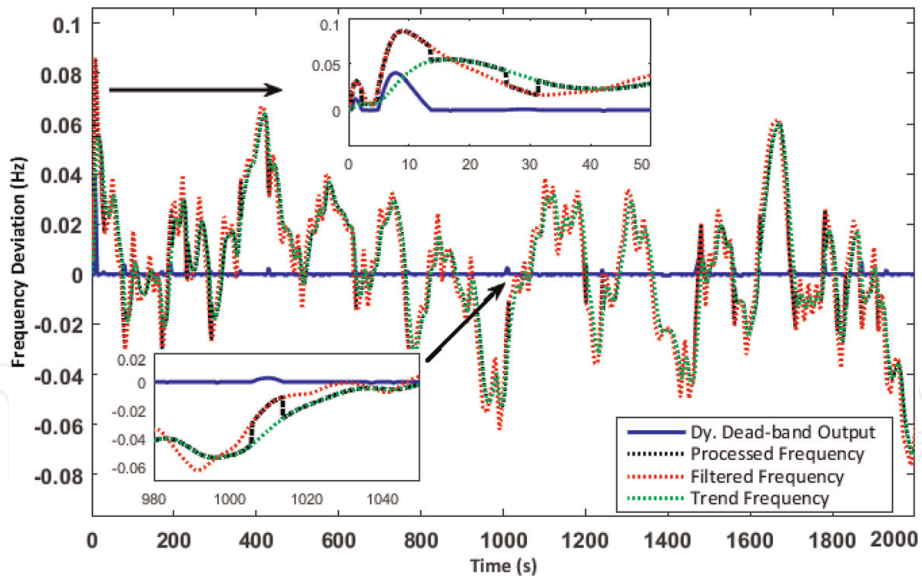


Figure 4.  
 Grid frequency vs. processed frequency at different threshold values (presented in different colors).

## 2.4 Frequency response controller model-I

Frequency response controller model-I as shown in **Figure 8** incorporates basic frequency processor in its structure to provide frequency response operation. This frequency controller block can provide two types of frequency response according





**Figure 5.** Processed frequency, trend filter output, low-pass freq. Filter output, and DDB output when threshold applied is  $>0$ .

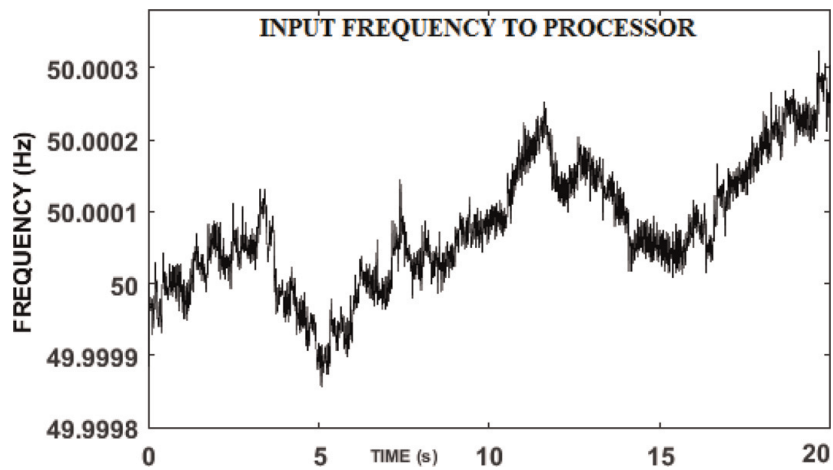


**Figure 6.** An example of input frequency obtained from NEM 14-generator model provided as input to frequency processor.

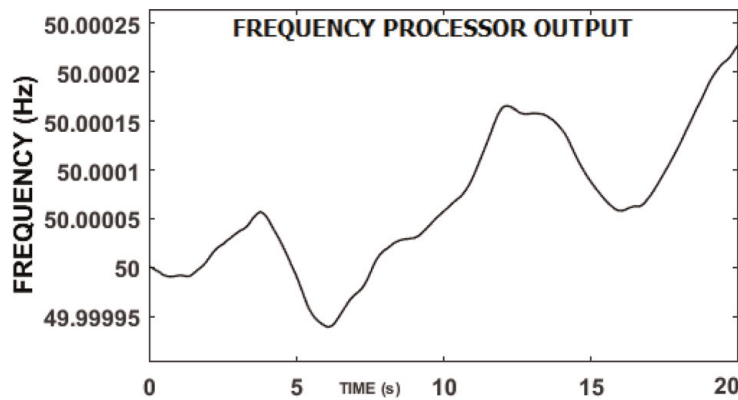


**Figure 7.** NEM 14-generator model processed frequency obtained from grid frequency processor.

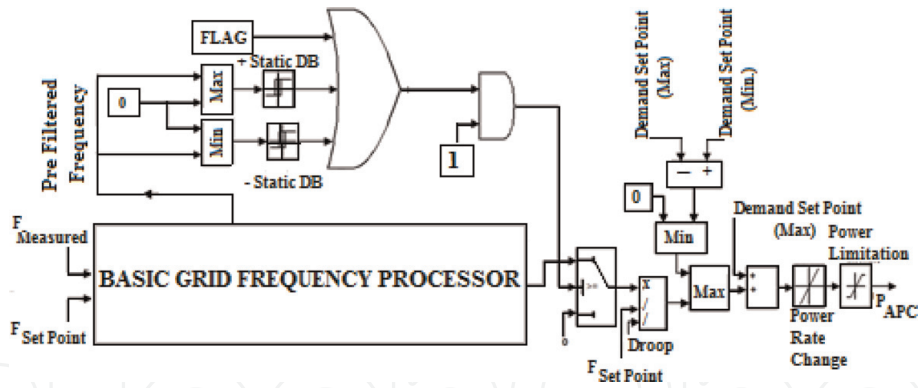


Figure 8.  
 Frequency response controller model-1.

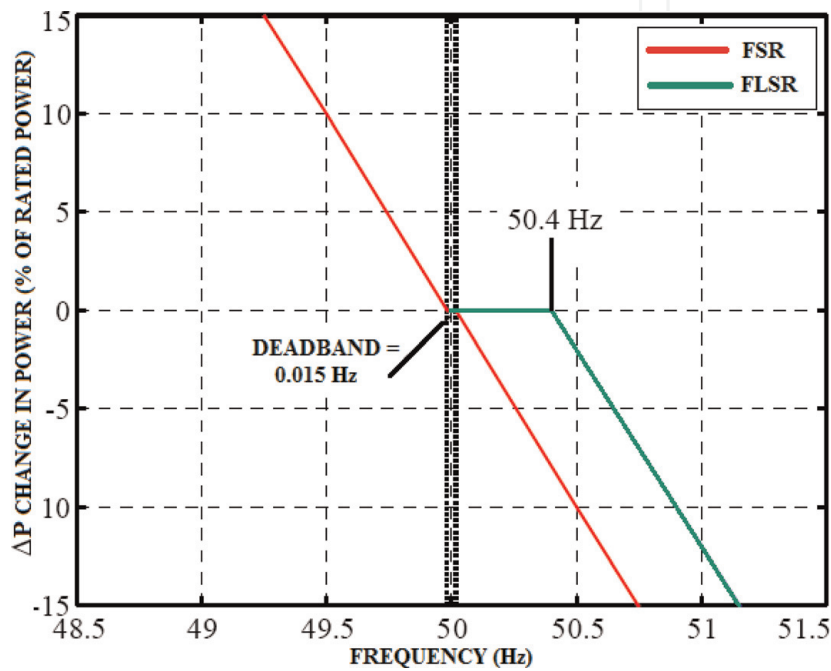


Figure 9.  
 Frequency grid code UK [35].

to the grid code as shown in **Figure 9**. Algorithm of this frequency response controller is explained through the flowchart given in **Figure 10**.

#### 2.4.1 Frequency-sensitive response mode

By setting FLAG equal to 1, frequency-sensitive response mode can be activated. Power set point will change proportionally to both up and down frequency deviation from reference frequency signal. Processed output frequency is generated through the coordination of the trend control frequency signal and dynamic dead-band. If measured frequency follows trend control frequency signal within dynamic dead-band, trend frequency signal is forwarded for generating droop power response; otherwise measured frequency signal is forwarded. VSWTG final active power set point is generated through an algorithm implemented on frequency response power and power demand set point.

#### 2.4.2 Frequency limited sensitive mode

By setting FLAG equal to 0, limited frequency-sensitive response mode can be activated to provide high-frequency response. There should not be any power

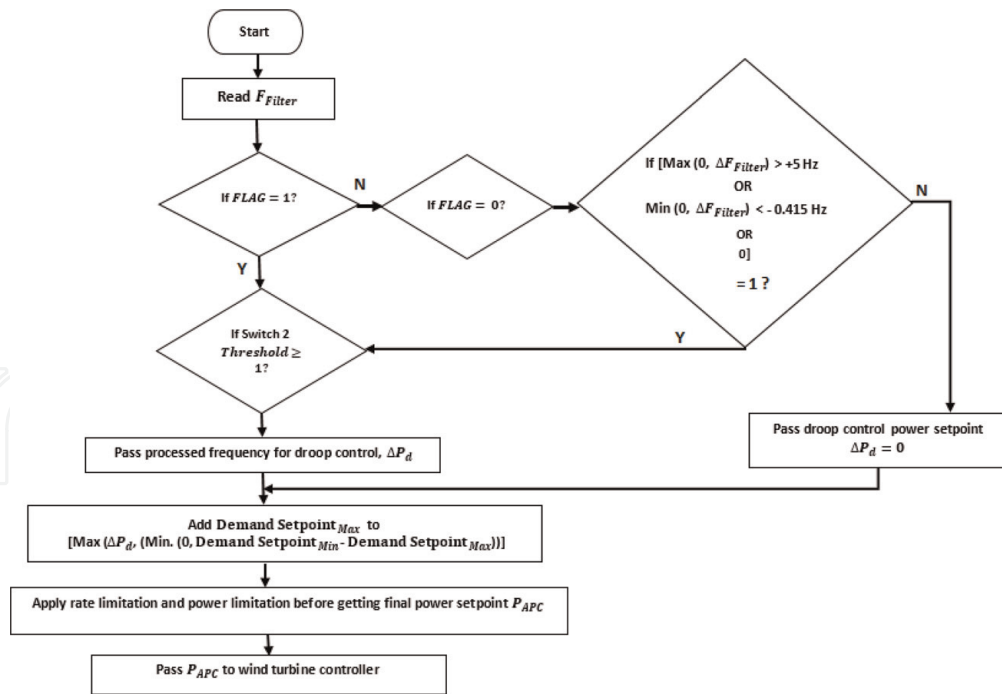


Figure 10. Algorithm for frequency controller-I FSR and FLSR response.

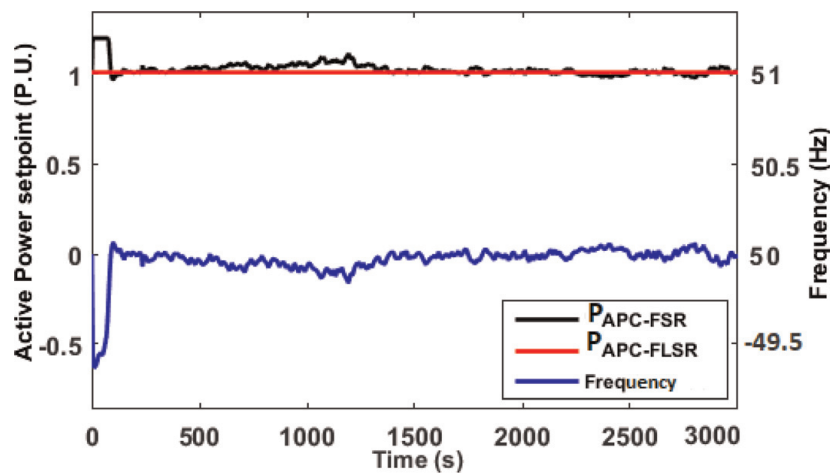
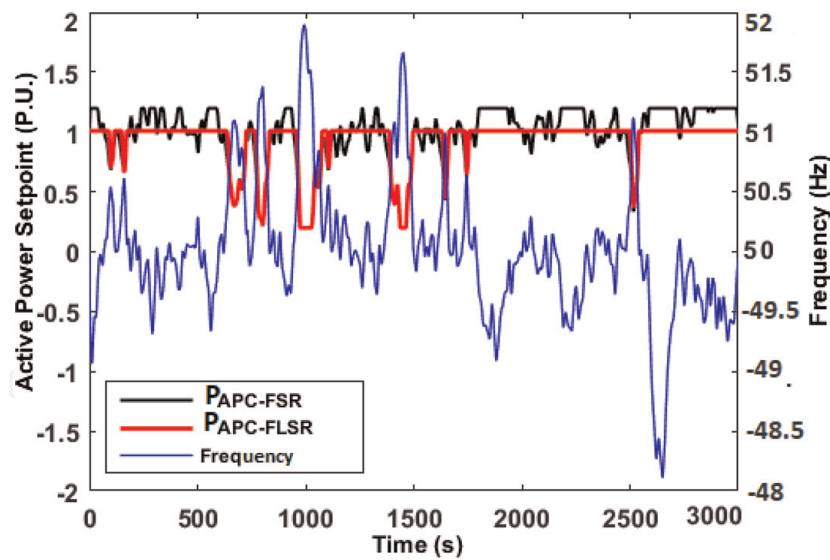


Figure 11. Example of frequency controller-I FSR and FLSR response.

variation corresponding to the frequency changes except when the frequency exceeds the upper limit. Insensitive mode incorporates a static dead-band around the frequency set point. If frequency error remains within static band, trend frequency signal and dynamic dead-band has no influence on output power.

Frequency response operation of the controller-I can be understood by **Figures 11** and **12**. As shown in **Figure 11**, when working under frequency-sensitive mode, wind frequency response controller-I provides high active power set point in case of low system frequency and low active power set point in case of high frequency. In limited frequency response mode, frequency response controller-I provides only low active power set point when system frequency is more than 50.4 Hz for reduced power generation. In case of frequency being lower than 50.4 Hz, wind turbine follows the demand set point as shown in **Figure 12**. This type of frequency controller is highly compatible with grid codes like that of the UK and Australia which requires full response from wind farms under normal conditions and limited up/down response under high-frequency conditions.



**Figure 12.**  
 Another example of active power set point generated when employing frequency response controller-I in two different modes.

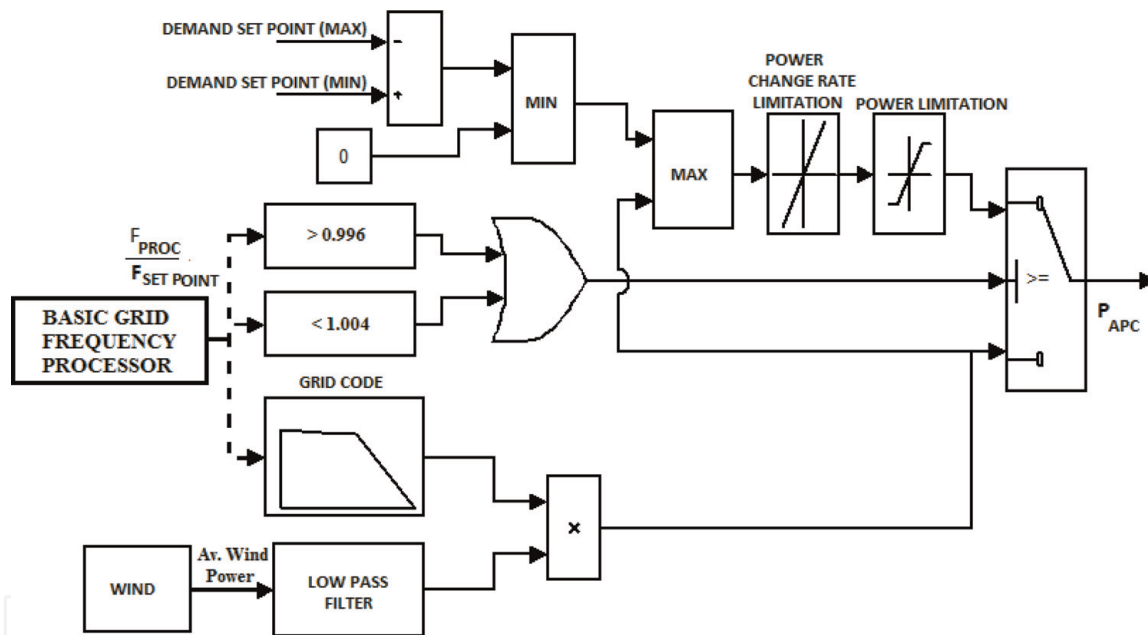


**Figure 13.**  
 Frequency response controller model-II.

## 2.5 Frequency response controller model-II

Frequency control model as shown in **Figure 13** implements the setting of active power set point according to typical nonsymmetrical droop curve very similar to Irish grid code as shown in **Figure 14**. Wind speed and processed frequency from basic frequency processor block are its two inputs. A wind profile module is implemented to provide variable wind speed as given in **Figure 15** for this study. The available wind power in per unit (p.u.) is calculated as a function of wind speed:

$$P_{avail} = \frac{1}{2} \rho A V^3 \quad (2)$$

where  $P_{avail}$  is the wind power [W],  $\rho$  is the air density [ $\text{kg}/\text{m}^3$ ],  $v$  is the wind speed [m/s], and  $A$  is the swept area [ $\text{m}^2$ ] of rotor disk that is perpendicular to the

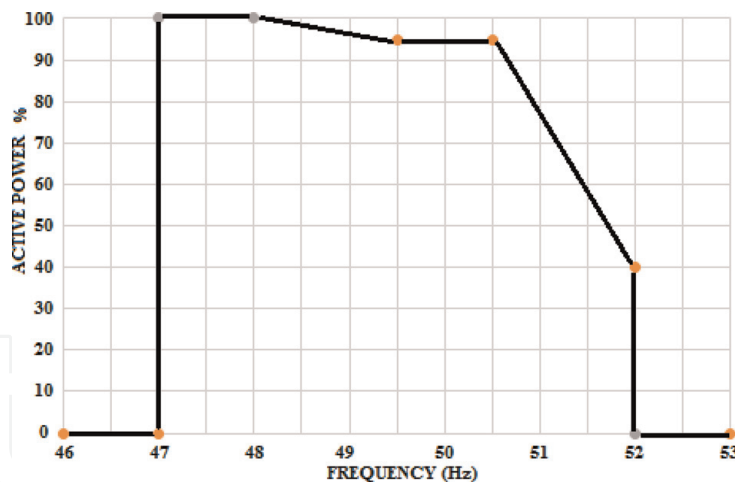


**Figure 14.**  
Nonsymmetrical droop curve for frequency power regulation.

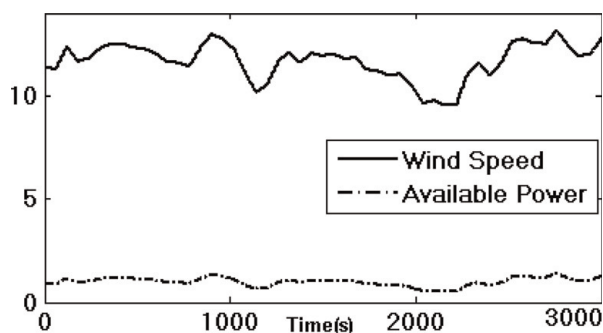


**Figure 15.**  
Variable wind speed (m/s) and available wind power (p.u.) as applied in this study.

wind flow [36]. Filtered available wind power is then multiplied with the power set point received from algorithms defining respective grid codes for incoming frequency. Power set point is then compared with maximum and minimum power restrictions to generate final active power set point. Limited set point is achieved when additional condition is imposed as IF frequency variation  $< 0.996$  AND frequency variation  $> 1.004$ ,  $P_{set-point} = P_{avail} \times P_{Grid-code}$ . Implementation of this restriction helps in maintaining maximum output from wind turbine in case of limited deviation. Flowchart of this controller is given in **Figure 16**.

A wind power plant is running as spinning reserve will produce less power at all wind speeds, thereby always providing a power reserve. Grid code controller will act as spinning reserve controller to vary the WPP grid power production as per transmission system operator request. In the case of wind farm operation, turbine set point can be multiplied by active power demand provided by farm controller to generated frequency-responsive power demand. **Figure 17** shows various power set points generated through grid code compatible frequency controller-II at variable wind speed and fluctuating grid frequency. Black color is the power set point required according to an example grid code, while green is the available wind power. This available power is multiplied with grid code power and limited, thereby providing a reserve power to be used in frequency deviations. We can notice that VSWTG electrical power output follows the limited active power set point provided from the frequency controller.

## 2.6 Variable speed wind turbine generator generic model

Type 3 and type 4 variable speed wind turbine generator VSWTG generic models adopted from [37] are applied in studying frequency-responsive active

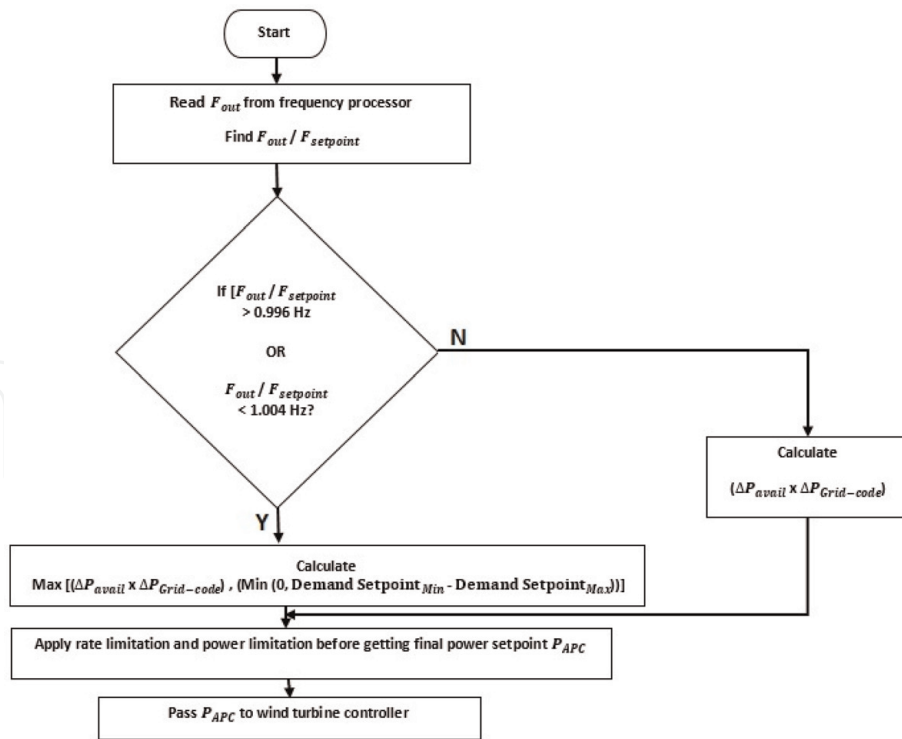


Figure 16. Flowchart depicting algorithm for frequency response controller model-II.

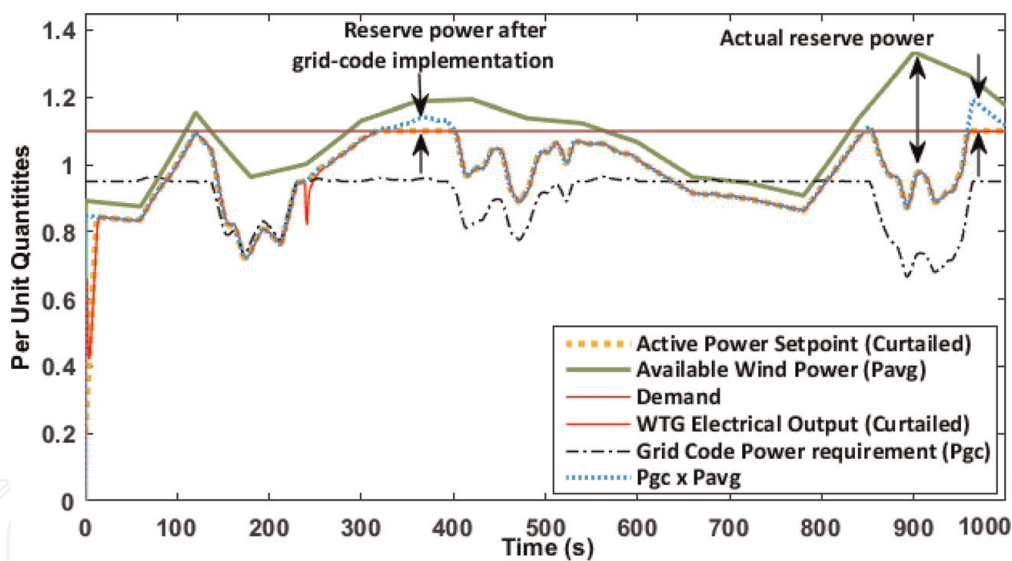
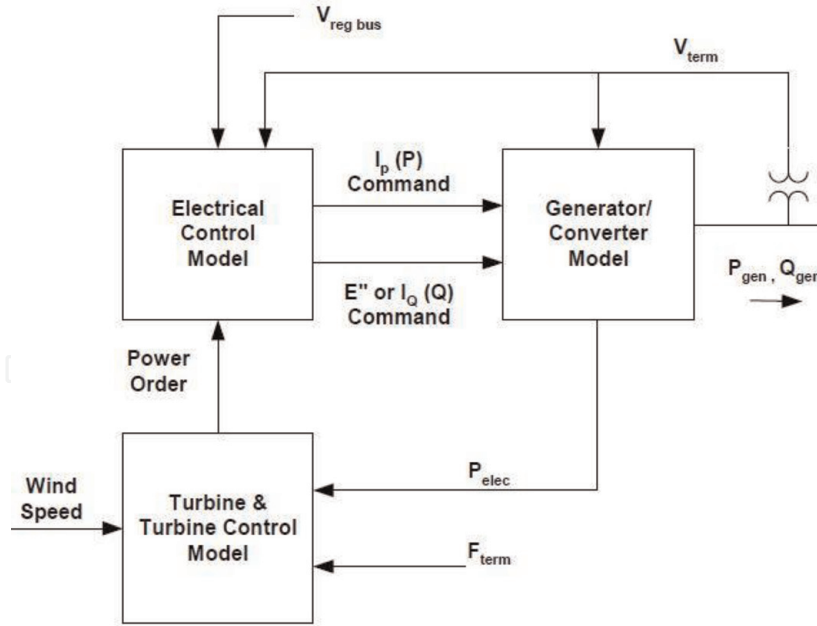


Figure 17. VSWTG power set points with limited power set point as grid controller output set point and corresponding generated power.

power control. Generic models of both type 3 and type 4 VSWTG have three basic blocks as shown in **Figure 18**: turbine model, generator/converter model, and electrical control model. Detailed model of these blocks can be obtained from [37, 38]. With all similar components and parameters, the major distinguishing factors between type 3 and type 4 VSWTG are in terms of electrical control model. Type 3 electrical control model is represented by flux and active current command, while type 4 electrical control model generates a reactive current command also along with active current command and includes a dynamic braking resistor and converter current limit. During frequency response, real power has priority, so detailed reactive power loop is not applied in both models in this study. The turbine control system in both type 3 and type 4 frequency-responsive models has the common



**Figure 18.**  
Modular model for variable speed wind turbines.

objective of controlling power production while maintaining rotor speed below minimum limit. Generic turbine control involves two control loops which receive speed error as input and deliver two control outputs: (1) wind turbine reference power order provided to the converter electrical control and (2) pitch reference value to pitch controller. Rotor speed is controlled as per power command through torque limitation in speed control loop. The current study applies a modified wind turbine control loop which is shown in a red dotted line. One mass lumped mechanical shaft model and detailed aerodynamic model as given in [38] are applied in these models (**Figure 19**).

Power order from torque controller is altered by passing grid code frequency-responsive active power set point  $P_{APC}$  through power response rate limiting block. Different gain values are applied to torque controller in type 3 and type 4 VSWTG and provided in the Appendix. Rotor speed error is given as input to both these controls. Final power order ( $P_{final-ord}$ ) is generated by adding grid code limited active power set point from frequency response controller block to difference between active power limited set point power and power order from speed controller ( $P_{APC} - P_{inp}$ ) and can be represented as

$$P_{final-ord} = P_{APC} + \left( \frac{sT_w}{1 + sT_w} \right) (P_{APC} - P_{inp}). \quad (3)$$

Ramp rate is implemented by including a washout filter whose time constant ( $T_w$ ) is detrimental to rate limit imposed on changes in power order. Wind turbine regulates the electrical power according to frequency-responsive final power order ( $P_{final-ord}$ ). A combined torque-pitch control method utilizing  $P_{APC}$  is applied in this study to obtain reserve power mode operation. Pitch compensation block provides the necessary margin for frequency-responsive option in current study. Pitch compensation block takes ( $P_{APC}$ ) generated from frequency-responsive controller instead of rated 1 p.u. reference power. Mechanical power and corresponding shaft speed of wind turbine is controlled through pitch controller and pitch compensation loop. Pitch controller enables control of aerodynamic wind power by rotor blade pitching in order to regulate turbine torque. Maximum power of 1.2 p.u.

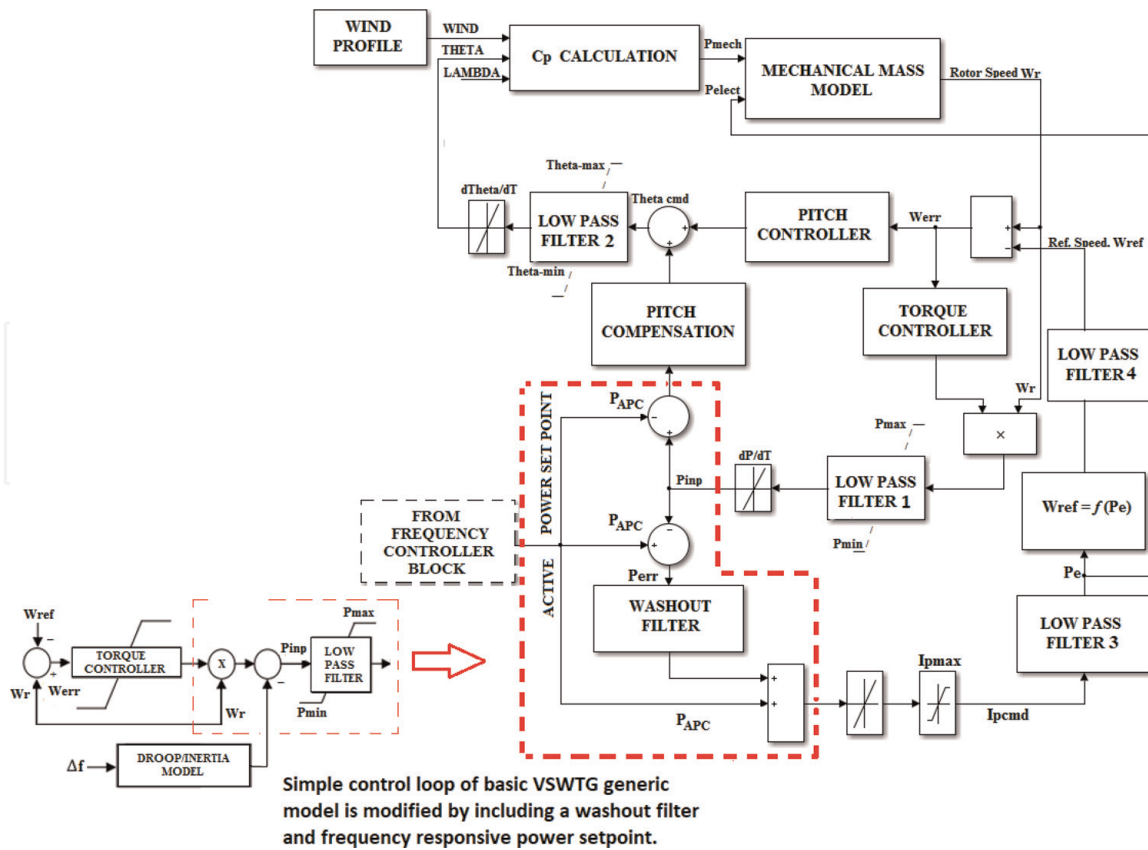


**Figure 19.** Type 3 VSWTG model with active power controller feeding power set point PAPC to power controller loop, pitch controller loop, and speed controller loop.

is available at zero pitch angle, while it is highly reduced with the highest pitch angle. Pitch angle is obtained through a series of proportional integral (PI) regulator and mathematically expressed by the following equations:

$$\theta_{cmd} = \frac{d(K_{ip}(\omega - \omega_{ref}))}{dt} + \frac{d(K_{ic}(P_{max} - P_{set}))}{dt} + K_{pp}(\omega - \omega_{ref}) + K_{pc}(P_{max} - P_{APC}) \quad (4)$$

If  $0.15 \text{ p.u.} \leq P_{elect} \leq 0.75 \text{ p.u.}$ , Then  $\omega_{ref} = -0.79131P_{elect}^2 + 1.526046P_{elect} + 0.49188$ .

Else If  $P_{elect} \geq 0.75 \text{ p.u.}$ , Then  $\omega_{ref} = 1.2 \text{ p.u.}$

Else If  $P_{elect} \leq 0.15$ ,  $\omega_{ref} = 0.689 \text{ p.u.}$

More details about the model and components can be referred from [37, 38] (Figure 20).

In maximum power point tracking (MPPT) operating mode, turbine power set point is determined, such that

$$P_e = K_{opt}\omega_r^3 \text{ and } K_{opt} = \frac{0.5\pi R^5 \rho}{\lambda_{opt}^3} C_p(\lambda_{opt}, \beta_0). \quad (5)$$

During maximum power point tracking operational mode, wind turbine electrical power output  $P_e$  is equal to MPPT power set point  $P_{opt}$ , rotor speed  $\omega_{VSWTG}$  is equal to  $\omega_{opt}$ , and pitch angle  $\beta = \beta_0 = 0^\circ$ . When turbine switches from MPPT mode to commanded power mode, power set point  $P_{opt}$  changes to  $P_{final-order} = P_e$ . VSWTG power drops below mechanical power, thereby increasing rotor speed to





beyond rated values, final power order is limited to the optimum power value ( $P_{opt} = K_{opt}\omega_r^3$ ). The turbine will continue to run in MPPT mode unless there is a change in wind speed or change in active power set point from frequency controller. Active power set point from frequency controllers is limited as per desired reserve power of 10% in this study.

In reserve power mode operation, assume steady state condition represented by point *a* for blue curve at some wind speed such that turbine mechanical power equal to VSWTG electrical power  $P_e P_{final-order}$ . In the case of frequency deviation due to generation loss, frequency-responsive VSWTG's power will increase to compensate for this loss and may reach VSWTG rated capacity limit shown by point *b* in **Figure 21**. Power extraction due to kinetic energy will continue until rotor speed hits the minimum limit at point *d*. After this point, the mechanical power will be more than the electrical power, and rotor will again speed up to finally settle at point *e* with speed  $W_e$ . All interconnected grid code-compatible VSWTGs are required to ensure a fast pitch control as well as other mechanical controller to be able to participate in a frequency response services in an acceptable time.

## 2.7 Test system: single area load frequency control (LFC) model

Wind penetration in low inertia power systems or system with low primary frequency response has an adverse effect on frequency stability. In order to explore the frequency-responsive wind power plant footprints on the electrical grid frequency regulation performance, a single area load frequency control (LFC) system model using MATLAB/Simulink software is analyzed. Control area power system model as shown in **Figure 22** incorporates hydro power plant along with frequency-responsive wind farm. Detailed modeling of hydro power plant is given in [2]. Since the aim of current study is to assess the improvement provided by frequency-responsive VSWTG model, only a brief description on load frequency modeling is provided in this section. In conventional LFC system, frequency and active power output of generating plants including wind power plants in a single control area is related as

$$\Delta F(s) = [\Delta P_{Gen}(s) + \Delta P_{Wind}(s) - \Delta P_{Load}(s)] \frac{K_P}{1 + ST_P} \quad (6)$$

where  $T_P = \left(\frac{2 * H_{eq}}{D * f^0}\right)$  is defined as the power system time constant and  $K_P = \frac{1}{D}$  is the power system gain.

LFC operation is accomplished through integral controller, implementing flat frequency control which implies area control error (ACE) as change in frequency  $\Delta f$ .

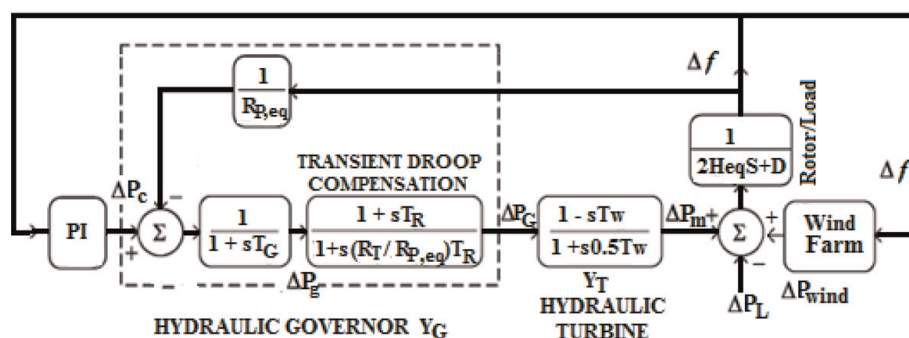


**Figure 22.** Single area hydro governor turbine model [2] with integrated wind farm.

$$ACE_i = \Delta f \quad (7)$$

$$\Delta P_{ci}(t) = -K_i \int (ACE_i) dt. \quad (8)$$

Changed droop setting according to wind penetration is given as

$$R_{new} = \frac{R_{old}}{1 - L_p}. \quad (9)$$

On a system-base value of 5000 MW and assuming 0.05 p.u. extra support from VSWTG during frequency excursions, wind-integrated system modified inertia constant,  $H_{eq}$ , is calculated as [16]

$$H_{eq} = H_{system}(1 - L_p) + H_{WT}L_p \quad (10)$$

$$H_{system} = \frac{\sum_i^N S_{ni} * H_i}{S_{system}}, \text{ where } S_{system} = \sum_i^N S_{ni}$$

where  $H_i$  and  $S_i$  are the inertia rating and apparent power rating of individual generating units and  $L_p$  is the wind penetration level. For frequency-responsive wind plant, wind inertia contribution  $H_{WT}$  to power system by providing  $\Delta P_e$  extra active power when system is subjected to step load disturbance  $\Delta P_L$  is calculated as

$$H_{WT} = \frac{\frac{-T_d D}{\ln X} - 2H_{eq}(1 - L_p)}{2L_p}; \quad (11)$$

$$X = e^{\frac{-T_d D}{2H_{eq}(1-L_p)}} \left( 1 - \frac{\Delta P_e L_p}{\Delta P_L} \right) + \frac{\Delta P_e L_p}{\Delta P_L}. \quad (12)$$

Total time delay  $T_d$  associated with hydro governor turbine model is calculated on the basis of delay theory originally given in [39]. Summation of governor time constant, valve motion delay time, and turbine response time delay results in total time delay at which minimum frequency deviation occurs after system disturbance. Value of  $T_d$  is calculated as 3.7814 s for hydro governor-turbine model with system parameters given in [16]. System simulations are performed and compared for LFC model with similar parameters but integrated with five different frequency-responsive wind plant model. A comparative study is made for frequency response and its indicators, effect on VSWTG electrical support, and corresponding rotor speed.

The following points have been implemented in this simulation study:

1. A constant load disturbance is applied.
2. All VSWTG models are provided with the same wind speed as shown in **Figure 15**.
3. Frequency response controller-I and frequency response controller-II are implemented for VSWTG model which are shown in **Figures 19** and **20**.
4. Same droop setting of 0.0315 p.u. MW/p.u. Hz is used for all individual generators including hydro and wind plants.
5. Equivalent droop setting of area 1 changes with wind penetration. A 10% wind penetration is used in simulation.

6. The same system inertia is applied in control area model.

All simulation parameters including LFC system parameters are provided in the Appendix.

### 3. Results and discussions

#### 3.1 Comparison of frequency controller response

Frequency-sensitive response is studied for step load change and with/without considering available wind power in power set point generation algorithm. In **Figure 23a, b**, it can be noticed that for any frequency variation outside the dead-band limit, there is a change in active power set point, and VSWTG tracks this power set point with some delay. When available wind power is not considered in algorithm, output power set point tracks demand set point. To investigate the effect of the available wind on frequency controller-I FSR output, power set point algorithm is modified such that

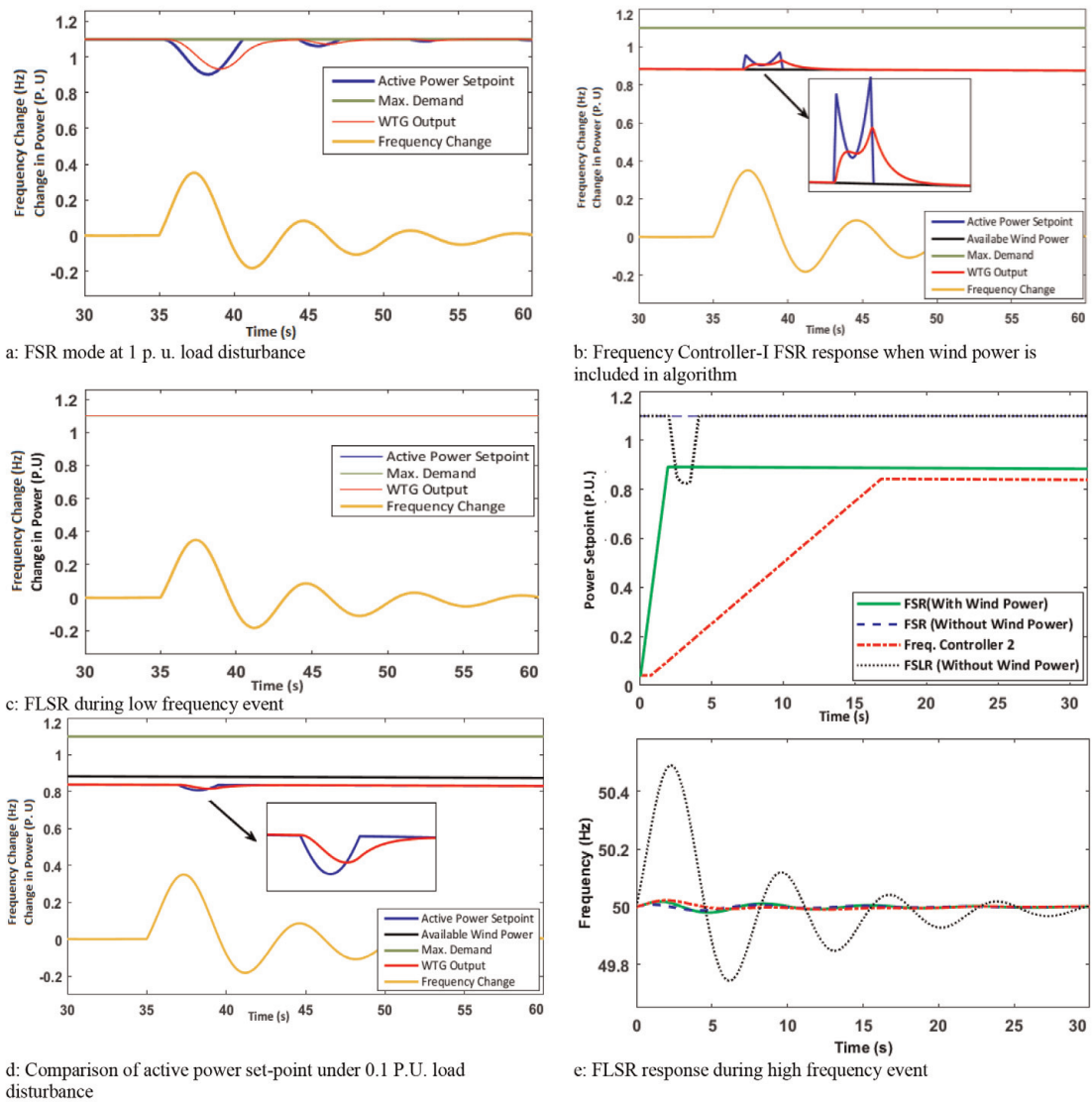
$$\text{If } \left( \frac{F_{Grid}}{F_{set-point}} > 0.996 \right) \text{ AND } \left( \frac{F_{Grid}}{F_{set-point}} < 1.004 \right), P_{set-point} \text{ EQUALS } P_{avail-wind},$$

else power set point is set as per the algorithm shown in flowchart.

In can be seen in **Figure 23b** that power set point tracks available wind power during normal frequency variation but changes during frequency disturbance. Its value then depends upon maximum value out of droop power or demand set points. VSWTG output traces the provided power set point, but inclusion of wind power can add to significant delay in VSWTG processing. **Figure 23c** shows the frequency-sensitive limited response where a constant power set point is provided if frequency deviation is within a set limit. Frequency-sensitive limited response is provided in the form of power set point variation only when the frequency deviation is more than the set limit: 50.4 in current study. **Figure 23e** shows the frequency-sensitive limited response when frequency increases above 50.4 Hz in the form of decreased power set point from frequency controller. **Figure 23d** presents the frequency controller-II response. Unlike frequency controller FSR response, where power set point tracks the demand set point, frequency controller-II power set point is highly dependent upon grid code power requirement, available wind power, and demand set points. It can be noticed that under all similar parameters and limitation, VSWTG output during frequency disturbance is reduced when wind power is considered in algorithm.

#### 3.2 Comparison of frequency-sensitive type 3 and type 4 VSWTG response

Control area frequency variation under the effect of frequency controller-based wind plants is analyzed in this section. Type 3 and type 4 VSWTG electrical output and rotor speed are also presented when operating under frequency-sensitive power set point. **Figure 24a and b** gives the system frequency when 10% penetration of frequency-sensitive grid code compatible type 3 wind plant is integrated along with hydro plant. Maximum frequency drop is 49.99 Hz for 0.01 p.u. load disturbance, while it increases up to 49.83 Hz for 0.1 p.u. load disturbance. The best frequency response under low load condition is observed for frequency controller-II-based type 3 VSWTG integration, while at higher load disturbance, frequency nadir point


**Figure 23.**

Comparison of frequency controllers' response for step load change. (a) FSR mode at 1 p.u. Load disturbance. (b) Frequency controller-I FSR response when wind power is included in algorithm. (c) FLSR during low-frequency event. (d) Comparison of active power set point under 0.1 p.u. load disturbance. (e) FLSR response during high-frequency event.

is slightly increased under wind power and variable droop-based frequency controller-II. Frequency nadir point is nearly the same when type 3 VSWTG is working under frequency controller-I. Frequency controller-II performance in terms of frequency nadir point is slightly deteriorated under type 4 VSWTG integration during low load condition as shown in **Figure 25a**. Electrical power output from both type 3 and type 4 VSWTG is reduced during frequency deviations under low and high load disturbances as shown in **Figures 24c, d** and **25c, d**. Respective power set points provided by frequency controllers are shown in **Figure 24e, f**. During the frequency disturbance, when electrical power support is provided from VSWTG models, rotor speed remains above the minimum limit of 0.7 p.u. for both types of VSWTG model as shown in **Figures 24g** and **25g**.

The reduction in power output is highly dependent upon active power set point algorithm based on available wind power and variable droop. Wind power calculation through manufacturer provided curve applies an oversimplified approach where wind power is modeled primarily as the cube function of hub height wind speed alone, while practically other factors like wind shear and turbulence are also involved [40, 41]. Wind power forecasting involves conversion of atmospheric

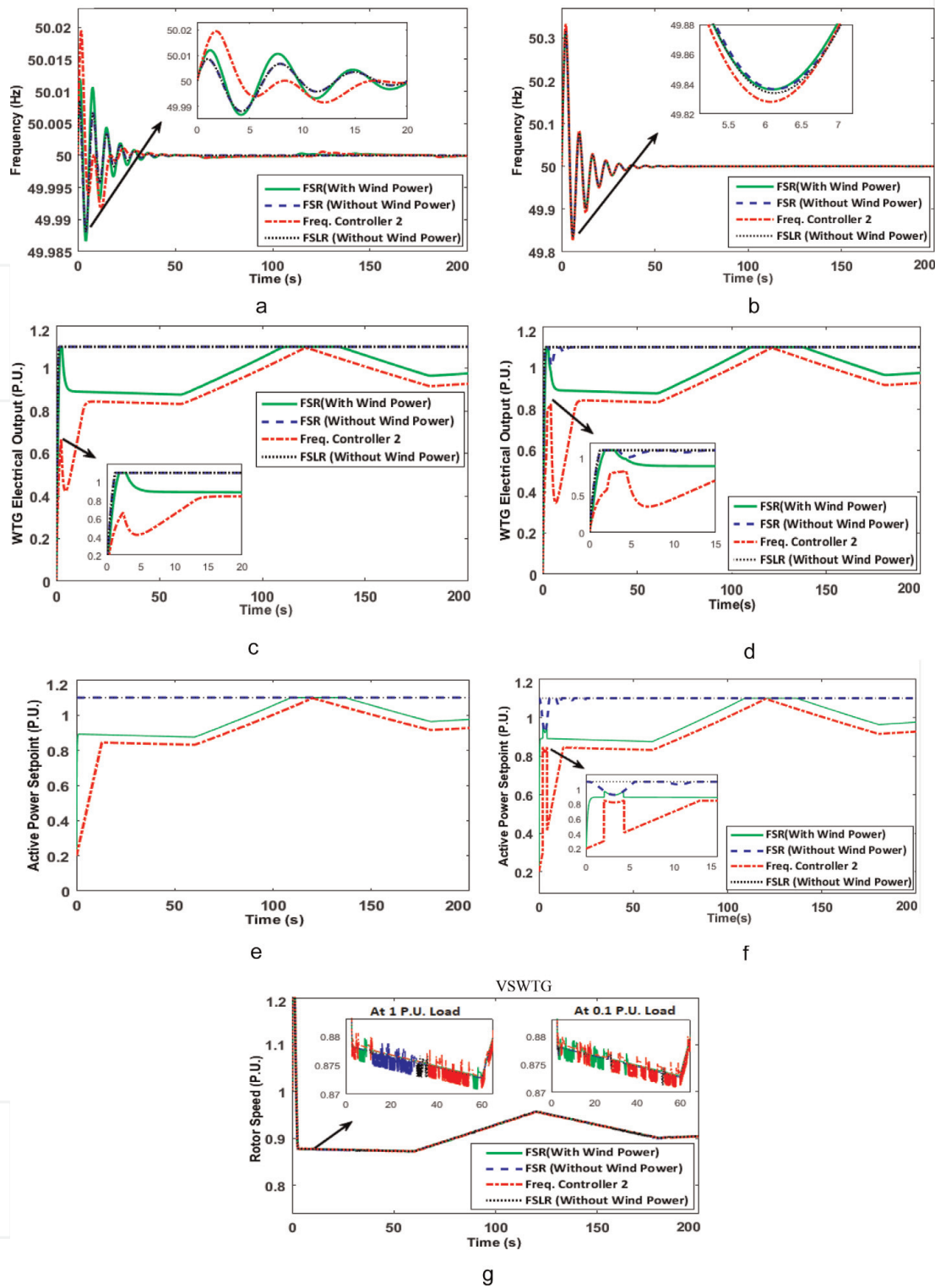


**Figure 24.** Type 3 VSWTG frequency-sensitive response during step load change. (a) Type 3 VSWTG frequency response at 0.1 p.u. load disturbance. (b) Type 3 VSWTG frequency response at 1 p.u. load disturbance. (c) Type 3 VSWTG electrical power at 0.1 p.u. load disturbance. (d) Type 3 VSWTG electrical power at 1 p.u. load disturbance. (e) Active power set point at 0.1 p.u. load disturbance for type 3 VSWTG. (f) Active power set point at 1 p.u. load disturbance for type 3 VSWTG. (g) Type 3 VSWTG rotor speed.

forecasts into turbine power output forecasts. Inaccurate measurement and forecasting may highly affect wind turbine output and turbine life. 20% error in wind speed forecasting may introduce around 41% error in wind power output [42]. Anticipation of actual wind energy at time horizon less than 1 min is hard as wind power forecasting involves a lot of uncertainty due to spatial and temporal variability of wind fields and different forecasting tools. Accurate wind power forecasts,

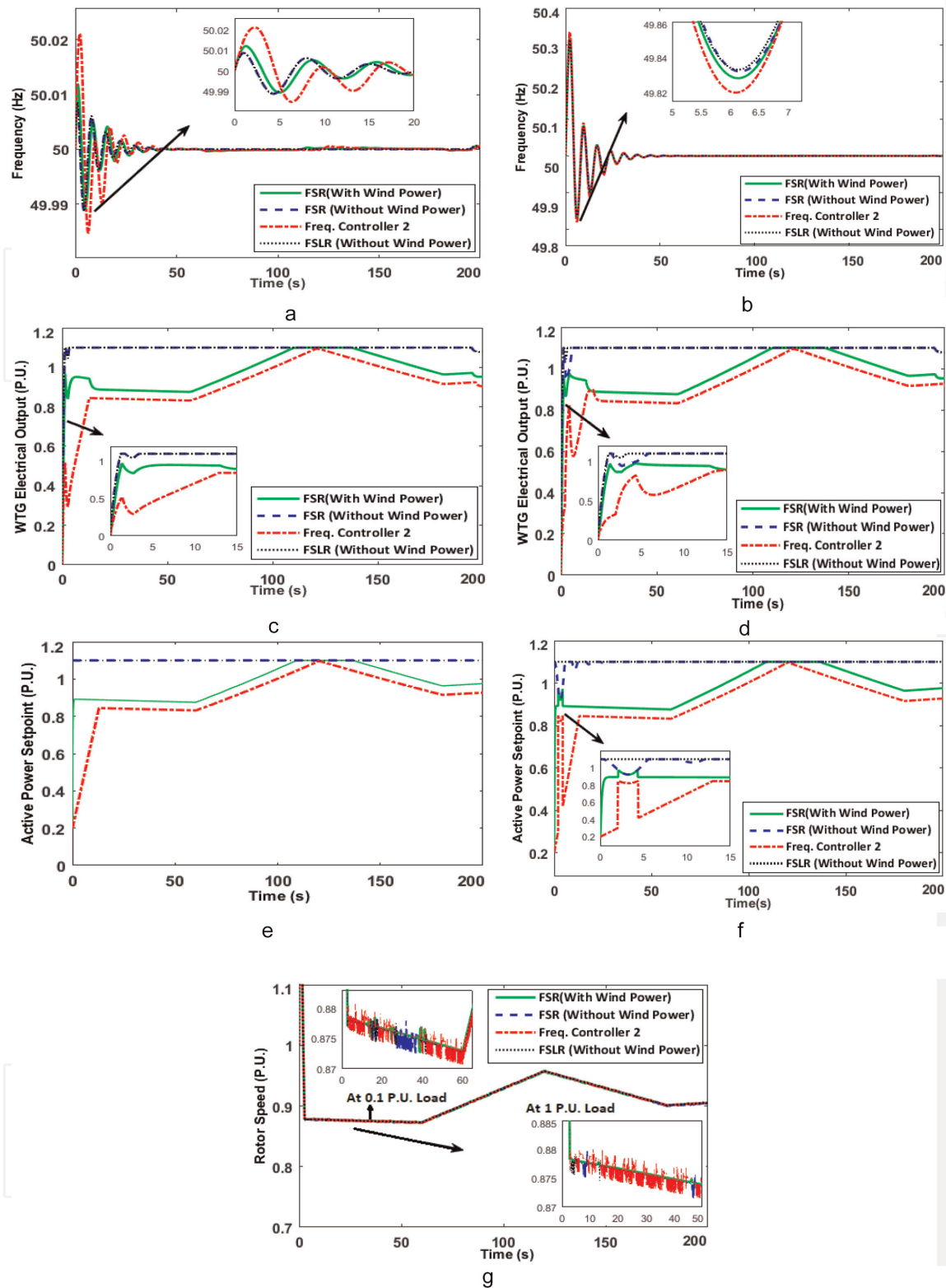


**Figure 25.** Type 4 VSWTG frequency-sensitive response during step load change. (a) Type 4 VSWTG frequency response at 0.1 p.u. load disturbance. (b) Type 4 VSWTG frequency response at 1 p.u. load disturbance. (c) Type 4 VSWTG electrical power at 0.1 p.u. load disturbance. (d) Type 4 VSWTG electrical power at 1 p.u. load disturbance. (e) Active power set point at 0.1 p.u. load disturbance for type 4 VSWTG. (f) Active power set point at 1 p.u. load disturbance for type 4 VSWTG. (g) Type 4 VSWTG rotor speed.

related uncertainty, and their corresponding effect on wind turbine controller are computationally challenging and require a multiscale simulation approach [41]. Integration of wind forecasting will significantly increase the processing time of the turbine controller.

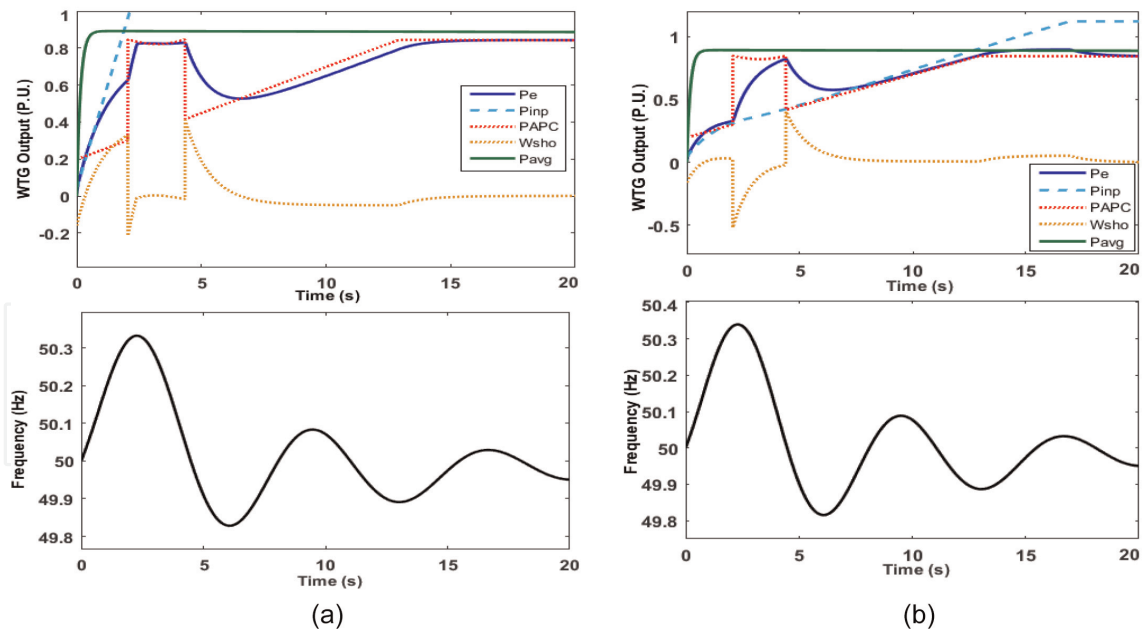


**Figure 26.** Comparison of type 3 and type 4 VSWTG model internal power orders during frequency disturbance. (a) Type 3 VSWTG outputs at 1 p.u. load disturbance. (b) Type 4 VSWTG outputs at 1 p.u. load disturbance.

The generic model of type 3 and type 4 are different mainly in terms of electrical control model and different gain values for torque controller. Type 4 VSWTG generic model includes braking resistance which has no impact during normal frequency disturbance, while the braking resistance absorbs excessive energy when power order is larger than delivered energy to the grid. There is slight variation in final electrical power order for type 3 and type 4 VSWTG when wind power is included in algorithm and is shown in **Figure 26**. Final electrical power order is also dependent upon internal power set points and washout filters which are shown in **Figures 19** and **20**. The turbine control model sends a power order ( $P_{imp}$ ) to the electrical control, requesting that the converter deliver this power to the grid. This power order is further altered by frequency-sensitive power set point ( $P_{APC}$ ). The electrical control may or may not be successful in implementing this power order. **Figure 26a, b** shows the active power response of type 3 and type 4 VSWTG. Wind turbine final electrical order ( $P_e$ ) initially follows the power order  $P_{imp}$  but then starts following the frequency controller power order  $P_{APC}$  as soon the frequency crosses the threshold. The washout filter power response rate limit ( $Wsho$ , orange line) transiently allows the power order variations from the ( $P_{APC}$ , red) through to the final power order ( $P_e$ ). Due to the difference in torque controller gains and low-pass filter gain for type 3 and type 4 VSWTG, a comparatively faster matching response is observed for type 4 VSWTG control, where final electrical power order  $P_e$  jumps from minimum  $P_{imp}$  to maximum  $P_{APC}$  during frequency disturbance. Type 3 VSWTG control also closely follows the power order  $P_{APC}$  during frequency disturbance. Final power order  $P_e = P_{APC}$  at around 15 s for type 3 VSWTG and around 18 s for type 4 VSWTG

### 3.3 Comparison of frequency controller-based type 3 VSWTG model with other frequency-sensitive models

Frequency droop model-I [43], droop model-II [44], and inertia droop model [18] are incorporated in basic torque control loop-based type 3 VSWTG model [16] which is shown as inset in **Figure 19** for comparison with modified control loop-based VSWG response when provided with frequency-sensitive power set point.



**Figure 27** gives the frequency deviation obtained from single area controlled model with 0.1 per unit load disturbance. Due to frequency-responsive active power support from VSWTG, a clear improvement in area frequency deviation can be observed with proposed frequency-responsive VSWTG model integration. In single controlled area model, low-frequency deviation and low settling time of around 30–35 s are observed with frequency controller-based VSWTG integration. More overshoots and undershoots are observed for other droop-based VSWTG models and settling time of around 45–50 s. Superiority of grid code-compatible frequency response controllers is established through simulation results in terms of reduced settling time, improved ROCOF, and frequency nadir point.

Rate of change of frequency after a disturbance either due to load variation or generation imbalance is determined on the basis of system inertia and amount of imbalance and is given as

$$\frac{df}{dt} = \frac{-f_0}{2H_{conv}} * \Delta P \quad (13)$$

The management of ROCOF is critical to maintaining power system frequency within the frequency operating standard and to maintaining the power system in a secure operating state. The amount of inertia required to maintain a particular ROCOF under different contingency is proportional to the contingency size. Lower inertia leads to a higher ROCOF. That means the frequency changes faster following a disturbance in a power system with less synchronous generation, and this could result in the loss of additional generation or load to arrest the frequency deviation when it occurs. There is no TSO's control over minimum system inertia, but ROCOF has to be within certain limits as per grid code. ROCOF obtained under different load disturbance scenario and 10% wind penetration is given in **Figure 27c**. Though the values obtained cannot be held indicative of real-time scenario which has interaction between components of varying electrical characteristics, a clear improvement is observed in ROCOF values for control area when proposed frequency-based controller-based Type 3 VSWTG is integrated with hydro power plant. A more detailed system will be required to analyze actual ROCOF changes.

Frequency nadir after any contingency is detrimental to primary frequency regulation for maintaining system stability. The primary frequency reserve adequacy criterion can be expressed as [45]

$$Freq_{Nadir} = (\Delta P_{Load}, PrimaryFrequencyReserve, F_{db}) \geq Freq_{min}, \quad (14)$$

where  $\Delta P_{Load}$  is the maximum power loss during contingency,  $F_{db}$  (Hz) is the maximum governors' dead-band,  $Freq_{Nadir}$  is the frequency nadir after the loss of  $\Delta P_{Load}$ , and  $Freq_{min}$  is the minimum frequency required. Wind power plant integration and its participation in frequency regulation services can be analyzed through frequency nadir points achieved under different combinations. Frequency nadir obtained for different frequency-responsive VSWTG models integrated in control area is shown in **Figure 27d**. Frequency nadir point as achieved under different load disturbance scenario indicates the superiority of grid code compatible frequency controllers over normal droop-based VSWTG model.

An important point to notice about other three droop-controlled models is in terms of wind plant power output during and after frequency response in LFC model. **Figure 27e, f** shows the zoomed version of electrical power output from VSWTG with different droop-controlled models during the initial frequency deviation in control area. Even though a variable wind speed is applied in simulation, a constant wind speed of 11.3 m/s is observed during approximately 20 s of frequency deviation.

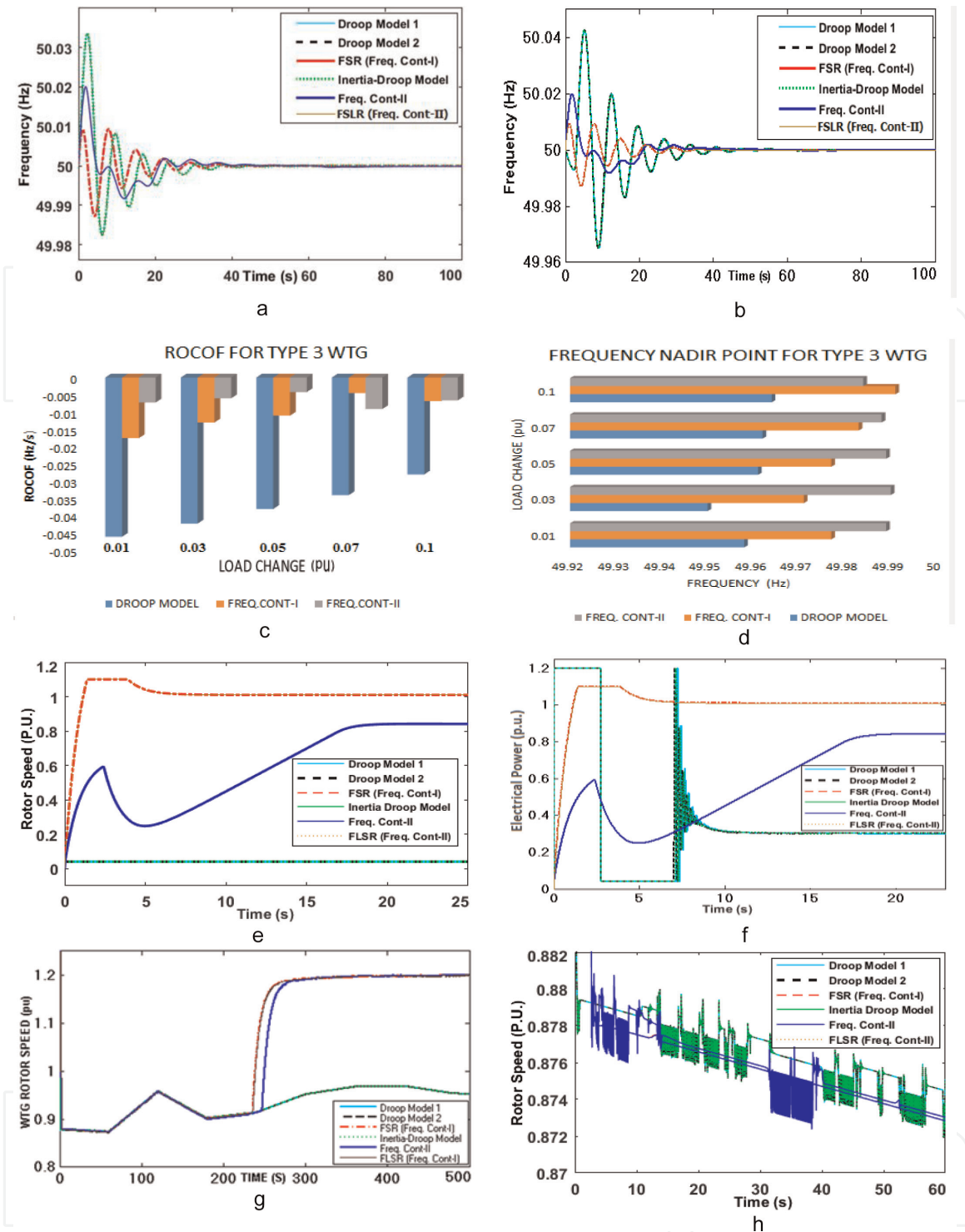


**Figure 27.** Comparison of type 3 VSWTG modified model with other droop-based models incorporated with basic VSWTG model. (a) Frequency response of single area LFC control model for 0.1 p.u. Load disturbance,  $Req = 0.035$  for all cases, torque controller gains (3, 0.6), no retuning applied for torque controller in simple VSWTG models. (b) Frequency response of single area LFC control model for 0.1 p.u. Load disturbance and  $Req = 0.035$  in all cases, torque controller retuned for other droop-based VSWTG models. (c) Rate of change of frequency (ROCOF) comparison for different load change (p.u.) and 10% VSWTG penetration. (d) Frequency nadir comparison for different load change (p.u.) and 10% VSWTG penetration. (e) Electrical power from type 3 VSWTG with no retuning of torque controller for 0.1 p.u. Load disturbance. (f) Electrical power from type 3 VSWTG with retuned torque controller for 0.1 p.u. Load disturbance. (g) VSWTG rotor speed variations during frequency response. (h) VSWTG rotor speed variations during frequency response (Zoomed).

Considering a 0.1 p.u. load disturbance and VSWTG provided 0.05 p.u. active power support, control area sees this frequency support from a machine with 3.4 s inertia constant. This inertia constant will change to 7.17 s if 0.1 p.u. of extra support from VSWTG is assumed. VSWTG will replace other conventional generation (having

equivalent inertia 6 s) if they provide an active power support of approximately 0.8 p.u. during frequency excursions. It can be observed that even with same load disturbance and same system inertia constant for all control areas, a different frequency response is obtained. All the three droop-based models attempt to provide increased electrical power up to 1.2 p.u. soon after detecting the frequency drop but fail to maintain net power output after frequency disturbance correction. Electrical power from basic VSWTG model finally settles at 0.4 p.u. as soon as frequency improves. This was also earlier confirmed in [16] and requires torque controller parameter retuning for increased electrical power after temporary frequency deviations.

We can notice a clear improvement in electrical power temporary support from VSWTG model incorporating frequency controller-I and controller-II. Following the active power set point generation algorithm, a constant active power set point equal to 1.01 p.u. is provided by frequency controller-I to ramp up the power during the moments of frequency deviations. Frequency controller-II also provides an increasing power reference set point of around 0.85 p.u. during the initial 20 s of frequency deviation and changes according to grid requirements and available power. VSWTG model with frequency controller-I is able to maintain electrical power around 1.1 p.u. during moments of initial frequency deviations, while VSWTG with frequency controller 2 has initial power drop up to 0.3 p.u. and then starts increasing and settles at around 1.1 p.u.

**Figure 27g, h** shows the change in rotor speed for Type 3 VSWTG model during frequency response in control area. All VSWTG models show reduced rotor speed maintained approximately 0.87 p.u. during those initial moments of frequency deviations till 20 s when extra electrical power from VSWTG is expected. Rotor speed of type 3 VSWTG with other droop models finally settles at around 0.95 p.u. with consequent reduced electrical output power to 0.4 p.u. Drop in rotor speed is observed due to imbalance in mechanical and electromechanical torque when electrical power is increasing for frequency controller-I and controller-II, but as soon as frequency deviation settles, an increase in rotor speed is also observed which settles at around 1.2 p.u. A minimum limit of 0.75 p.u. and maximum limit of 1.2 p.u. has been imposed in current studied VSWTG model.

#### **4. Conclusions**

There is an increasing demand for frequency control ancillary services due to high penetration of wind power plants in electrical network. This paper presented a modeling framework for frequency dependent active power set point generation in variable speed wind turbines and its corresponding effects on system frequency regulation response. Individual wind turbine can be made grid code frequency compatible by including additional active power set point generator output to the modified torque control loop of respective turbine. Active power set point generator applies designed power limitation on available wind power, rated turbine power, and TSO commanded power and provides set point to turbine. A grid frequency processor based on dynamic dead-band and moving averaged frequency filter is used to suppress noise frequency signals from passing to active power set point generator. Simulations were carried out for a single area control model with 10% wind penetration. Control area frequency responses as well as integrated VSWTG's electrical and rotor speed responses were compared with other frequency droop-based VSWTG model responses. Promising results in terms of improved settling time and better electrical power and rotor speed variations during frequency deviations were obtained for proposed frequency-responsive VSWTG model in comparison to other common droop-inertia-based model.

Grid processor presented in this study will be further improved and tested with low-pass IIR filter with a resettable strategy once measured frequency enters again. One per unit power limitation was applied in active power set point controller which will be further tested for more realistic power commands. Frequency response for area 1 was determined using classical linear hydraulic turbine model. It would be interesting to investigate the area frequency response with advanced inelastic nonlinear hydraulic turbine model interaction with frequency-responsive wind power plants.

## A. Appendix

### 1. LFC system parameters used in single area LFC simulation

$H_{\text{system}}$	$T_d$	R
6	3.7814	0.0315
$K_i$ (for single area model)	$P_L$ (p.u.)	$L_p$ (wind penetration)
-3.88	1-30%	10%

### 2. Droop model parameters

Inertia droop model: low-pass filter constant, 0.1 s; $K_{\text{inertia}}$ , $2 \cdot H_{\text{wind}}$ ; high-pass filter constant, 1 s; $K_{\text{droop}}$ , 0.0315
Droop model-1: low-pass filter constant, 0.01 s; washout filter constant, 6 s; droop, 0.0315
Droop model 2: low-pass filter constant, 0.2 s; $K_{\text{droop}}$ , 0.0315

### 3. Frequency grid processor parameters

Prefilter constant, 0.5 s; trend generator/filter constant, 8 s; upper dead-band, 0.015
Lower dead-band, 0.001; post filter constant, 0.5 s; droop, 0.0315

### 4. VSWTG parameters (differences are highlighted in bold)

Type 3 VSWTG (modified torque loop) with frequency response controller	Type 3 VSWTG (basic torque loop) with droop controllers
Aerodynamic model: $C_p(\lambda, \theta) = C_1 \left( \frac{C_2}{\lambda_i} - C_3 \theta - C_4 \right) e^{-\frac{C_5}{\lambda_i}} + C_6 \lambda$ $\frac{1}{\lambda_i} = \frac{1}{\lambda + 0.08 \theta} - \frac{0.035}{\theta^3 + 1}$ $c_1 = 0.5176, c_2 = 116, c_3 = 0.4, c_4 = 5, c_5 = 21, \text{ and } c_6 = 0.0068$ Pitch controller, $K_{pp} = 150, K_{ip} = 25$ ; pitch angle limitation, 0-27° Pitch compensation: $K_{pc} = 3, K_{ic} = 30$ <b>Inputs: <math>P_{APC}, P_{inp}</math></b> Low-pass filter 2 time constant: 0.3 s <b>Torque controller: <math>K_{ptrq} = 3, K_{itrq} = 0.6</math></b> Low-pass filter 4 time constant: 60s Power limitation: 0.04-1.1 p.u. <b>Washout filter constant: 1.0 s</b> Gen/converter model: Maximum current limitation: 1.1 p.u. Low-pass filter 3: 0.02 s	Aerodynamic model: -Same Pitch controller: same Angle limitation: same Pitch compensation, same; <b>Inputs, Pref = 1, <math>P_{inp}</math></b> <b>Torque controller: <math>K_{ptrq}, -271.5; K_{itrq}, -310.7</math></b> Low-pass filter (TC) constant: 5 s Power limitation: same <b>Washout filter not present</b> Gen/converter model: Maximum current limitation: 1.1 Low-pass filter: 0.02

---

Type 4 VSWTG has all the same parameters as that of Type 3 VSWTG	Type 4 basic VSWTG model has all the same parameters as that of modified loop-based type 4 VSWTG model except
Electrical control:	Pitch compensator taking $P_{ref} = 1$ as input
$E_{bst}$ (p.u.), 0.2; $K_{dbr}$ , 10	Low-pass filter time constant: 0.05 s
Torque controller: $K_{ptrq} = 0.3$ , $K_{itrq} = 0.1$	
Low-pass filter time constant: 4 s	

---

IntechOpen


IntechOpen

### Author details

Asma Aziz\* and Aman Than Oo  
Faculty of Science, Engineering and Built Environment, Deakin University,  
Australia

\*Address all correspondence to: asma.aziz@deakin.edu.au

### IntechOpen

© 2020 The Author(s). Licensee IntechOpen. Distributed under the terms of the Creative Commons Attribution - NonCommercial 4.0 License (<https://creativecommons.org/licenses/by-nc/4.0/>), which permits use, distribution and reproduction for non-commercial purposes, provided the original is properly cited. 

## References

- [1] AEMO. Power System Operations Event Report: Multiple Generator Disconnection and under Frequency Load Shedding. 2009. Available from: [aemo.com.au](http://aemo.com.au)
- [2] Kundur P, Balu N, Lauby M. Power System Stability and Control. New York: McGraw-Hill; 1994
- [3] Jonkman J, Butterfield S, Musial W, Scott G. Definition of a 5-MW Reference Wind Turbine for Offshore System Development, NREL/TP-500-38060. Golden, CO: National Renewable Energy Laboratory; 2009
- [4] Pourbeik P, Ellis A, Sanchez-Gasca J, Kazachkov Y, Muljadi E, Senthil J, et al. Generic stability models for Type 3 & 4 wind turbine generators for WECC, In: Power and Energy Society General Meeting (PES). IEEE; 2013. p. 1, 5, 21, 22
- [5] Sørensen B, Andersen B, Fortmann J, Johansen K, Pourbeik P. Overview, status, and outline of the new IEC 61400-27—Electrical simulation models for wind power generation. In: International Workshop on Large-Scale Integration of Wind Power into Power Systems as Well as on Transmission Networks for Offshore Wind Power Farms; 2011
- [6] WECC. WECC Wind Power Plant Dynamic Modeling Guide, WECC Renewable Energy Modeling Task Force. 2010. Available from: [renew-ne.org](http://renew-ne.org)
- [7] National Grid. Mandatory Frequency Response | National Grid [online]. 2016. Available from: <http://www2.nationalgrid.com>
- [8] AEMC. Feasibility of Fast Frequency Response Obligations of New Generators. 2017. Available from: <http://www.aemc.gov.au/getattachment/661d5402-3ce5-4775-bb8a-9965f6d93a94/AECOM-report-Feasibility-of-FFR-obligations-of-new.aspx>
- [9] de Almeida R, Lopes JP. Participation of doubly fed induction wind generators in system frequency regulation. IEEE Transactions on Power Systems. 2007; 22:944-950
- [10] Juankorena X, Esandi I, Lopez J, Marroyo L. Method to enable variable speed wind turbine primary regulation. In: International Conference on Power Engineering, Energy and Electrical Drives; 2009. pp. 495-500
- [11] Liserre M, C'ardenas R, Molinas M, Rodriguez J. Overview of multi-MW wind turbines and wind parks. IEEE Transactions on Industrial Electronics. 2011;58(4):1081-1095
- [12] Morren J, de Haan S, Kling W, Ferreira J. Wind turbines emulating inertia and supporting primary frequency control. IEEE Transactions on Power Systems. 2006;21(1):433-434
- [13] Gowaid I, El-Zawawi A, El-Gammal M. Improved inertia and frequency support from grid-connected DFIG wind farms. In: Power Systems Conference and Exposition (PSCE). IEEE/PES; 2011. pp. 1-9
- [14] Ma H, Chowdhury B. Working towards frequency regulation with wind plants: Combined control approaches. IET Renewable Power Generation. 2010;4(4):308-316
- [15] Hansen AD. Evaluation of Power control with different electrical and control concepts of wind farms. Technical Report. Roskilde, Denmark: Project UpWind; 2010
- [16] Ullah NR, Thiringer T, Karlsson D. Temporary primary frequency control support by variable speed wind turbines

- Potential and applications. *IEEE Transactions on Power Systems*. 2008; **23**(2):601-612
- [17] Tarnowski GC, Kjar PC, Sorensen PE, Ostergaard J. Variable speed wind turbines capability for temporary over-production. In: *IEEE Power & Energy Society General Meeting*; Calgary, AB; 2009. pp. 1-7
- [18] Ramtharan G, Ekanayake JB, Jenkins N. Frequency support from doubly fed induction generator wind turbines. *IET Renewable Power Generation*. 2007;**1**:3-9
- [19] Attya AB, Hartkopf T. Wind farms dispatching to manage the activation of frequency support algorithms embedded in connected wind turbines. *International Journal of Electrical Power & Energy Systems*. 2013;**53**:923-936
- [20] Hughes FM, Anaya-Lara O, Jenkins N, Strbac G. Control of DFIG-based wind generation for power network support. *IEEE Transactions on Power Systems*. 2005;**20**:1958-1966
- [21] Mauricio JM, Marano A, Gomez-Exposito A, Ramos JLM. Frequency regulation contribution through variable speed wind energy conversion systems. *IEEE Transactions on Power Systems*. 2009;**24**:173-180
- [22] Gautam D, Goel L, Ayyanar R, Vittal V, Harbour T. Control strategy to mitigate the impact of reduced inertia due to doubly fed induction generators on large power systems. *IEEE Transactions on Power Systems*. 2011; **26**:214-224
- [23] Aziz A, Shafiullah GM, Stojcevski A, MTO A. Participation of DFIG based wind energy system in load frequency control of interconnected multi generation power system. In: *Power Engineering Conference (AUPEC)*. Perth, WA: Australasian Universities, 2014. pp. 1-6
- [24] Conroy JF, Watson R. Frequency response capability of full converter wind turbine generators in comparison to conventional generation. *IEEE Transactions on Power Systems*. 2008; **23**(2):649-656
- [25] Grunnet JD, Soltani M, Knudsen T, Kragelund MN, Bak T. Aeolus toolbox for dynamics wind farm model, simulation and control. In: *European Wind Energy Conference and Exhibition, EWEC 2010: Conference Proceedings*; 2010
- [26] Aho J, Buckspan A, Laks J, Fleming P, Jeong Y, Dunne F, et al. A tutorial of wind turbine control for supporting grid frequency through active power control. In: *Proceedings of the 2012 American Control Conference*, Montreal; 2012
- [27] Janssens NA, Lambin G, Bragard N. Active power control strategies of DFIG wind turbines. In: *2007 IEEE Power Tech*, Lausanne; 2007. pp. 516-521
- [28] Tarnowski GC, Kjær PC, Dalsgaard S, Nyborg A. Regulation and frequency response service capability of modern wind power plants. In: *Proceedings of the Power and Energy Society General Meeting*, 25–29 July 2010. Minneapolis, USA: IEEE; 2010
- [29] Hepner S, Wihler A. Method for controlling an output of an electrical power plant. US6118187 A; 2000
- [30] Smith S. *The Scientist and engineer's Guide to Digital Signal Processing*. San Diego, CA: California Technical Publications; 1997
- [31] ERA, 2014 ancillary service standards and requirements study, EY report to the Independent Market Operator, 2014. Available from: [www.erawa.com.au/cproot/14770/2/EY%20Final%20Report.pdf](http://www.erawa.com.au/cproot/14770/2/EY%20Final%20Report.pdf)

- [32] EY. Ancillary Service Standards and Requirements Study, Perth. 2014. Available from: [wa.aemo.com.au](http://wa.aemo.com.au)
- [33] North American Electric Reliability Council. NERC OPERATING MANUAL. NERC; 2004. Available at: [http://quantlabs.net/academy/download/free\\_quant\\_institutional\\_books\\_/\[NERC\]%20NERC%20Operating%20Manual%20-%20June%202004.pdf](http://quantlabs.net/academy/download/free_quant_institutional_books_/[NERC]%20NERC%20Operating%20Manual%20-%20June%202004.pdf)
- [34] Gibbard M, Vowles D. Simplified 14-Generator Model of the SE Australian Power System. South Australia: The University of Adelaide; 2008
- [35] The Grid Code. Issue 4, Revision 10. nationalgridESO. GC0110: LFSM-O compliance requirements for Type As and B PGMs, Stage 02: Workgroup Report. 2019. UK: National Grid Electricity Transmission PLC; 2012. Available at: [www.nationalgrideso.com/document/117576/download](http://www.nationalgrideso.com/document/117576/download)
- [36] Manwell J, McGowan J, Rogers A. Wind Energy Explained: Theory, Design and Application. Chichester: Wiley; 2011
- [37] Clark K, Miller NW, Sanchez-Gasca JJ. Modelling of GE Wind Turbine-Generators for Grid Studies, Version 4.5. General Electric International, Inc; 2010
- [38] Aziz A, Maung Than Oo A, Stojcevski A. Full converter based wind turbine generator system generic modelling: Variations and applicability. Sustainable Energy Technologies and Assessments. 2016;14:46-62
- [39] Chan ML, Dunlop RD, Schweppe F. Dynamic equivalents for average system frequency behaviour following major disturbances. IEEE Transactions on Power Apparatus and Systems. 1972; PAS-91(4):1637-1642
- [40] Miller W, Heller A. Breath of Air. In: Meteorological Technology International Journal. U.K. 2015. p. 22. Available from: <http://www.mbw.ch/wp-content/uploads/2015/05>
- [41] Str.llnl.gov. Predicting Wind Power with Greater Accuracy [Online]. 2017. Available from: <https://str.llnl.gov/april-2014/miller>
- [42] Sharman H. Why wind power works for Denmark. Proceedings of the Institution of Civil Engineers: Civil Engineering. 2015;158(2):66-72
- [43] Mauricio JM, Marano A, Gómez-Expósito A, Martínez Ramos JL. Frequency regulation contribution through variable-speed wind energy conversion systems. IEEE Transactions on Power Systems. Feb. 2009;24(1): 173-180
- [44] Yingcheng X, Nengling T. System frequency regulation in doubly fed induction generators. International Journal of Electrical Power & Energy Systems. 2012;43(1):977-983
- [45] Chavez H, Baldick R, Matevosyan J. The joint adequacy of AGC and primary frequency response in single balancing authority systems. IEEE Transactions on Sustainable Energy. 2015;6(3):959-966